The Effects of Conformal Symbology on Drivers' Visual Search

Master of Science Thesis

By

Marc Alexandre Schotman

TU Delft Delft University of Technology

Faculty of 3mE, Cognitive Robotics

The Effects of Conformal Navigation Symbology on Drivers' Visual Search

MASTER OF SCIENCE THESIS

Marc Alexandre Schotman

4223195

To obtain the degree of

Master of Science
In Mechanical Engineering

At the
Department of Cognitive Robotics
Delft University of Technology

Supervisors:
Prof. dr. ir. J. C. F. de Winter
Dr. ir. Y.B. Eisma
August 9th, 2021

TU Delft Delft University of Technology

Assessment Committee

Committee Chair
Dr. ir. Y. B. Eisma
Department of Cognitive Robotics
Faculty of 3mE, TU Delft

Supervisor
Prof. Dr. ir. J. C. F. de Winter
Department of Cognitive Robotics
Faculty of 3mE, TU Delft

External Member
Dr. ir. D. Dodou
Department of Medical Instruments & Bio-Inspired Technology
Faculty of 3mE, TU Delft

Student
M. A. Schotman
Department of Cognitive Robotics
Faculty of 3mE, TU Delft

PREFACE

I want to dedicate this preface to the special people I have in my life and who have supported me all this time. Firstly, I want to thank my mother, for her unconditional love and absolute selflessness. Not only during these slightly more difficult times, but through-out my life. Thank you, I love you so very, very much. I also want to thank my father, although he was not physically here, just thinking about him has always given me strength. It's difficult to express how much you have meant to me. There is so much I learned from you; you always gave me so much love. I'm truly blessed to have had parents like the two of you.

I also want express special gratitude to Thomas Booij, for the tremendous support you have given me the past years. You were always there to celebrate when times were good but also when times were 'less' good. It was an amazing pleasure to have you around. Furthermore, I want to thank my brother and all my other friends for hearing me vent my struggles and for lifting my spirits all too often. Mich, Lucci, Joe, Siets, Irene, and many more. Thank you all, I needed every single one of you. Last, but certainly not least, I want to thank my supervisors Yke and Joost. For making time for me when I needed them and for their professional advise through-out the entire process. I most definitely could not have done this without your help.

Marc Schotman
Augustus 9th, 2021

CONTENTS

The Effects of Conformal Navigation Symbology on Drivers' Visual Search

M. A. Schotman
Cognitive Robotics Dept., Faculty of 3mE, Delft University of Technology

***Abstract*—Driving often requires dividing attention between scanning the environment and following navigation instructions. The aim of this study was to investigate the effects of conformal and non-conformal navigation symbology on drivers' visual search. A driving simulator study was conducted where participants drove with conformal and non-conformal navigation symbology while performing an active visual search task consisting of detecting visual stimuli. The stimuli were highly transparent, yellow spheres projected on the side of the road. Eighteen participants drove three trials using different navigation symbology while their eye-movements were being recorded. Results showed a significant reduction in miss rate by 14% (from 44% to 38%) and a significant increase in mean fixation duration on visual stimuli by 16% (from 227 ms to 263 ms) when using conformal symbology. Eye-movements had a trend to be calmer during the use of conformal symbology indicated by lower saccade lengths. Furthermore, subjective ratings showed a clear preference for the conformal symbology. The findings of this study provide additional evidence for the benefits of conformal symbology within an automotive context, showing drivers to have an improved ability to sample the outside scene.**

***Index Terms*—Conformal Symbology, Visual Search, Eye-Tracking, Virtual Reality, Driving Simulator, Navigation Aid**

I. Introduction

Augmented Reality (AR) systems major strength is their capability of fusing virtual and real objects in the same space. Drivers can intuitively read the content of presented information by the virtual objects' location, shape, size, and colour; this type of representation is referred to world-fixed, contact-analogue, and *conformal* symbology. Conventional textual and graphical representations which do not relate to the environment on which they are projected are referred to as *non-conformal* symbology. Many studies within the aviation sector have measured positive effects on reaction speed, flight path error, and event detection when pilots used conformal symbology compared to non-conformal symbology [2, 12, 24, 33, 47, 49].

Drivers must often obtain information about their route while simultaneously keeping track of events and objects in the environment. Facilitating this divided attention task is one of the factors which must be considered when designing route guidance symbology. The intuitive nature of conformal symbology stems from its logical shape and location with respect to the environment on which it is projected e.g., highlighting lane boundaries or the to-be-followed road. However, such visual projections directly in drivers' direct field of view should be introduced cautiously as to not induce unforeseen negative drawbacks like occlusion, distraction, or interference with the visual processing of the outside scene [11, 41]. Therefore, a Virtual Reality (VR) driving simulator will be used to measure the effects of navigation symbology type on drivers' visual search, with a specific emphasis on the comparison of conformal and non-conformal symbology.

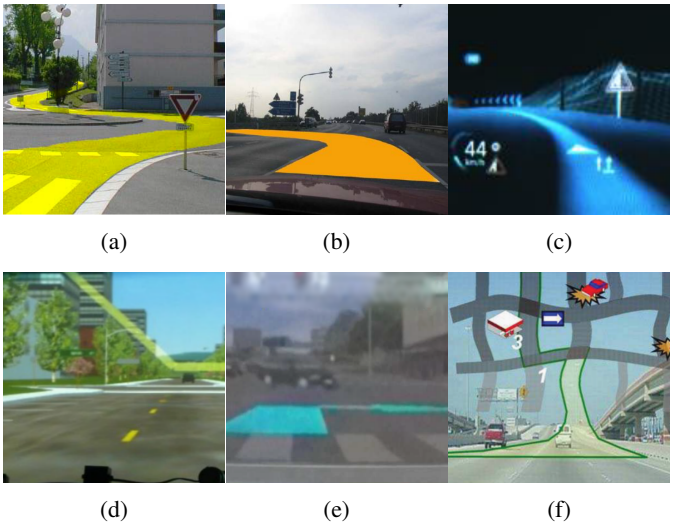

Fig. 1: Six examples of conformal navigation symbology: (a) by Narzt et al. [36], (b) by Poitschke et al. [37], (c) by Lee et al. [30], (d) by Medenica et al. [34], (e) by Gabbard et al. [15], and (f) by SeungJun and Anind K. [40]

A. Conformal symbology

Gish and Staplin [16] defined conformal symbology as:*" ... visual transformations of external objects to give observers the perception that the symbology is genuinely part of the external scene"*. For example, a 2-dimensional arrow would be non-conformal, whereas it would be conformal if the arrow were transformed continuously and dynamically, such that it looks as if it was part of regular road signage. Most research comparing conformal and non-conformal symbology has been performed in the aviation sector. Fadden et al. [12] performed a meta-analysis of 6 of such studies showing a consistent positive effect on flight path tracking and event detection (events occurred in both the environment and on the display) when using conformal symbology compared to non-conformal symbology. Moreover, Boston and Braun [2] showed benefits of conformal symbology to become more prevalent with increased complexity of the environment. In

comparison to pilots, drivers encounter much more complex environments and much more events within the environment. Therefore, it seems feasible that drivers would benefit even greater from the use of conformal symbology [14, 16].

Recent advancements in head-up display (HUD) technology have increased the potential display size and contributed to reduced costs [20] making HUDs more suited for regular consumer vehicles and for displaying conformal symbology. A multitude of different conformal navigation symbology have been proposed [30, 36, 37], their designs are illustrated in Figure 1. A few studies measured the effect of these conformal navigation system on drivers. For example, it has been shown that older drivers especially benefit from conformal navigation symbology, significantly reducing navigation errors, saccade length, and gaze speed while increasing relative dwell time on the road [34, 40]. The studies also contained conflicting results with reports of both an increase [15] and decrease [40] of mean fixation duration and number of fixations; and reports of positive [34, 40] and negative [13, 15] subjective measures. Note, that these conflicts are most likely due to the differences in symbology design, see Figure 1. However, none of the studies reported measures which represented drivers' ability to abstract information from the outside scene by means of an event detection or a visual search task.

B. Measuring drivers' visual search

Visual search of drivers has been measured by numerous studies in a variety of ways [3, 4, 8, 17, 19, 28, 39, 42, 43, 46]. Often, visual search is analysed using eye-movement measures like mean fixation duration, number of fixations, variation of fixation angles, saccade lengths, gaze speeds, and areas of interest analysis [3, 4, 8, 28, 43]. However, drivers' visual search can be measured by performance on a visual search task [17, 19, 29, 31, 46]. A visual search task always requires drivers to search for an object while driving, these can be real objects like landmarks or traffic signs [19, 42], or artificial objects inserted in a simulation, video footage, or secondary display [17, 29, 31, 46]. Eye-measures can give insight in the gazing pattern and has been used to distinguish novice and experienced drivers [27, 43, 44]. However, a visual search task can give a more direct measure of drivers' performance and is therefore used in this study alongside the regular eye-measures.

C. Driving simulators

Driving simulators have several advantages in comparison to on-road studies. Simulator-based studies are much cheaper, have an increased level of experimental control, and measuring eye-movements and driver input is easier. However, assessing the results of simulator-based studies on driver interfaces, especially AR-based ones, must be done with care because it is difficult to obtain realistic luminance contrast levels [35]. Additionally, driver behaviour will not be the same within a simulated environment since there are no risks involved [38]. These caveats must be considered when drawing conclusions or extrapolating results from simulator-based studies.

D. Eye-tracking in Virtual Reality

Recording eye-movements has traditionally put large constraints on participants head-movements requiring their heads to remain still through-out the duration of the experiment. VR based eye-tracking eliminates these constraints almost entirely, only requiring participants to wear a head-mounted display (HMD). Eye-tracking in VR is relatively new, first appearing in literature at the start of this millennium [7]. It offers a range of new possibilities for research on human perception and behaviour because it allows for participants' full head motion while tracking their gaze within a relatively naturalistic environment that reacts to their movements and actions. It also allows for easy tracking of objects of interest, recording the total dwell time, and number of fixations on specific objects. Additionally, the distance towards the point of fixation is easily traceable, giving an extra dimension to the conventional fixation measure. Clay et al. [6] showcases a range of experimental possibilities using eye-tracking in a VR environment.

E. Present study

The present study sought to evaluate the effect of conformal and non-conformal navigation symbology on drivers' visual search. Participants drove predetermined routes in a VR driving simulator using different types of navigation symbology while their eye-movements were tracked. Participants' visual search was measured by a set of eye-measures and by their performance on a visual search task. The ultimate goal of this study is to contribute to driver safety by examining whether conformal symbology can enhance drivers' ability to sample the environment.

II. Method

This experiment utilised a VR driving simulator to evaluate the effect of conformal and non-conformal navigation symbology on drivers' visual search. Participant drove three trials with three different navigation conditions. Their visual search was measured using both eye-movements and performance on a visual search task. Participants' eye-movements were recorded using the built-in eye-tracker of the HMD. From the eye-movements the following measures were extracted: fixation rate (fixations per second), fixation duration, saccade length, horizontal and vertical variation of gaze angle, and the horizontal and vertical gaze speed. Performance on the visual search task was measured by the miss rate of and reaction time to the visual stimuli.

A. Participants

Nineteen participants volunteered to participate in this experiment, 6 women and 13 men, with an average age of 26.7 and a standard deviation of 9.3. All had a legal drivers' license and drove at least once a month.

B. Apparatus

The environment was presented to participants using the Varjo VR-2-Pro, a high-resolution virtual reality glass equipped with two 1920 x 1080 low persistence micro-OLEDs, two 1440 x 1600 low persistence AMOLEDs, 90 Hz 20/20 eye-tracking, and hand-tracking. A Logitech G27 steering wheel, firmly attached to the table, was used for controlling the vehicle and for reporting detections during the visual search task.

C. Stimuli

The simulation environment was constructed using the game engine Unity, version 2019.4.3f1 and was based on the environment of Bazilinskyy et al. [1]. The environment consisted of connected intersections in an urban setting with static objects being present e.g., houses, lanterns, parked vehicles. Four different tracks were designed, all containing 12 left turns, 12 right turns, and 2 straights i.e., navigation operations. For each track the order of navigation operations was randomized, and miscellaneous objects were manually changed to reduce repetitiveness. Each track required around 6 minutes to complete.

Acceleration of the simulated vehicle was automated i.e., participants were only able to steer the vehicle. Automated acceleration was an attempt to equalise participants' exposure time to visual stimuli of the visual search task, exposure time to navigation instructions, and total driving time. If participants took a wrong turn, they were informed through an in-game interface about the error, the vehicle was stopped, and its position reset to 20 m before the intersection where the error occurred.

All participants drove each of the four tracks in the same order while the order of the navigation conditions was counterbalanced. The first track functioned as a practise track; participants were shown the three navigation conditions; they could become comfortable with the VR environment; practise with steering the vehicle; and practise with the detection button required for the visual search task. A more comprehensive description and technical details concerning the simulation can be found in Appendix D.

Fig. 2: Enclosed in each green bounding box is a visual stimulus. The visual search task required participants to search for these stimuli and report a detection using a button on the steering wheel.

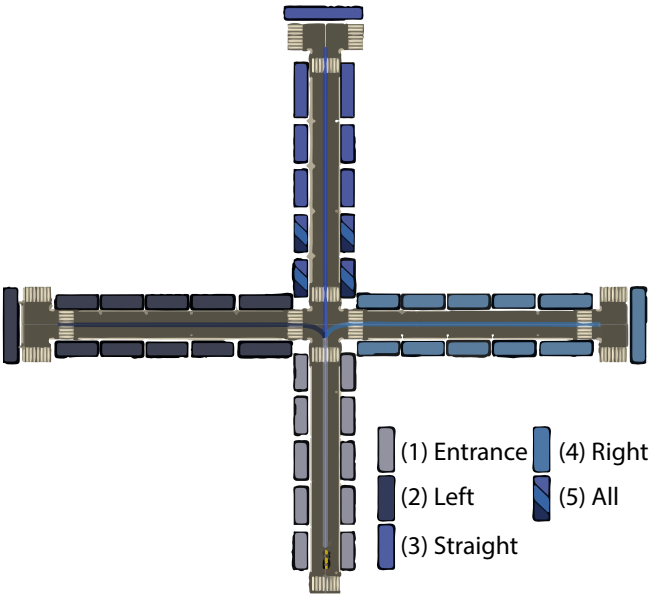

Fig. 3: Possible positions of visual stimuli for an intersection per navigation operation. For example, when the route proceeded left at the intersection, possible stimuli positions were at colour codes 1, 2, and 5.

D. Visual search task

The visual search task consisted of detecting low saliency stimuli, stimulating active visual search of the environment. They consisted of yellow spheres with a transparency of $2/255$ and a radius of 0.75 m, see Figure 2. The transparency and radius of the visual stimuli were based on the results of a preliminary experiment where six participants drove a multitude of trials with different transparencies and radii ranging from 25 to 1 and 1 to 0.5 m, respectively.

Each track contained 75 visual stimuli positioned in the areas depicted in Figure 3, with no more than one stimuli per area. Additionally, a minimum of 2 and a maximum of 5 stimuli were presented between each navigation operation i.e., per colour coded area in Figure 3. The position of stimuli were randomly generated for each of the four tracks once and thereafter used for all participants.

To report a detection, participants were required to look at the visual stimulus and press a button on the steering wheel. However, multiple visual stimuli would often be within the field of view of participants. Gaze vectors i.e., origin and direction of participants' gaze, were available to the simulation environment on a frame-by-frame basis. This information was used to determine which stimulus was being detected at the time of a button press. When a detection was reported, a stimulus was marked as detected if: (1) the gaze vector pointed directly at the stimulus during this frame; or (2) it was the most recently looked at stimuli within half a second of the

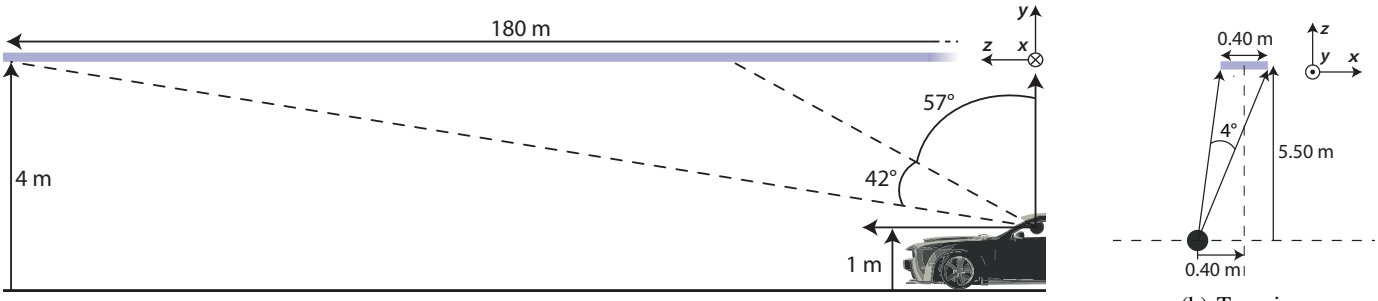

(a) Side view

(b) Top view

Fig. 4: Conformal symbology position and visual angles with respect to the driver. The visual angles were calculated for a driver of 1.85 m, with a seat-to-eye length of 80 cm, sitting 30cm from the steering wheel. The longest straight part of the simulation was 180 m which was therefore the maximum possible size of the conformal symbology.

current frame. After a stimulus was marked as detected it would disappear from the environment functioning as feedback for the participant.

The preliminary experiment which determined the radius and transparency of the visual stimuli is described in Appendix A. Also, a more detailed description of visual stimuli positioning and the specific implementation within the simulation, can be found in Appendix D.

E. Navigation conditions and symbology

The conformal symbology was inspired by Medenica et al. [34] and consisted of a translucent cable suspended 4 m above the road following the navigation route, from now on referred to as the virtual cable. Other designs were considered inspired on other works, see Figure 1, but a review of these systems revealed them to be impractical either due to being unintuitive or distracting. Therefore, they were not used during the experiment. The non-conformal navigation symbology were arrow representations of upcoming navigation operations i.e., arrows pointing left, right, or straight, with a distance indicator showing the remaining distance from the upcoming navigation operation. The non-conformal symbology was displayed on a HUD; positioned 2.5 m in front of the driver; measuring 20 cm high and 25 cm wide; similar to other HUD studies [21, 22, 26]. All navigation symbology were displayed using a semi-transparent, blue colour: RGBA(0, 0, 255, 100).

Three navigation conditions were employed during the experiment. One using the conformal virtual cable and two using the non-conformal arrow representations. The non-conformal conditions differed in their positioning of the HUD: a low positioned and a high positioned was used. The high positioned HUD was introduced to overlap the position of the virtual cable in order to exclude possible effects introduced by symbology position. The low HUD was introduced to validate participants use of the high positioned HUD. A high positioned HUD is unconventional and has been shown to be distracting [22]. Therefore, validating whether this high position was not affecting driver performance was deemed necessary. Appendix C contains a review of all conformal symbology designs considered for this study and a description of how the positions of

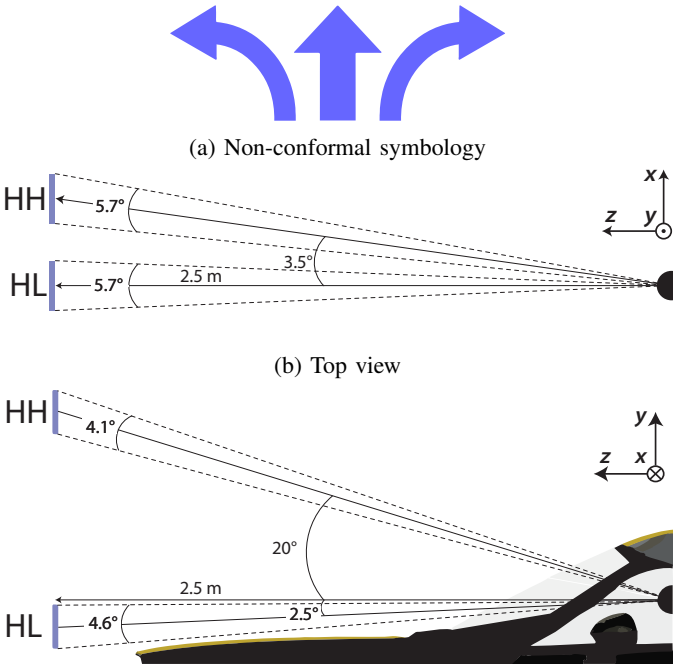

(a) Non-conformal symbology

(b) Top view

(c) Side view

Fig. 5: Non-conformal symbology and its position for the HL and HH conditions. The symbology was displayed on a 20 cm by 25 cm display at a horizontal distance of 2.5 m. The visual angles were calculated for a driver of 1.85 m, with a seat-to-eye length of 80 cm, sitting 30cm from the centre of the steering wheel. These images are not to scale.

the low and high HUD were determined. The three navigation conditions and their angles with respect to the driver are shown in Figures 4 and 5 and listed below:

1) Non-conformal symbology on a low HUD (HL): The symbology was displayed on a HUD, positioned 2.5 m in front of the driver, just above the hood of the vehicle, at a horizontal and vertical angle of 0° and -2.5°, respectively. The display spanned a horizontal and vertical visual angle of 5.7° and 4.6°, respectively.

2) Non-conformal symbology on a high HUD (HH): Similar to the HL condition, the symbology was displayed on a HUD, positioned 2.5 m in front of the driver, at a horizontal and vertical angle of 3.5° and 20°, respectively. This position coincided with the position of the virtual cable. The display spanned a horizontal and vertical visual angle of 5.7° and 4.1°, respectively.

3) Conformal symbology as a virtual cable (VC): The symbology was positioned at a height of 4 m, above the centre of the road, following the navigation route. It was rendered as a thin pipe with radius of 0.2 m. The symbology spanned a maximum horizontal and vertical visual angle of 4.1° and 42°, respectively.

F. Dependent variables

The following dependent variables were used to analyse drivers visual search: the fixation rate, as an indication of the drivers' sampling rate; mean fixation duration as measure of processing time; the variation of horizontal and vertical fixation angle to estimate the spread of visual search; mean saccade length and gaze speed as indications of search intensity; and the miss rate and reaction time during the visual search task to measure drivers' visual search capacity. Also, subjective ratings were gathered using the van der Laan Acceptance Scale [45]. The dependent variables were defined as follows:

(i) *Fixation rate (#/s)*: The number of fixations per second.
(ii) *Fixation duration (ms)*: The time spent during a fixation.
(iii) *Saccade length (°)*: The travelled angular distance between two successive fixations.
(iv) *Horizontal and vertical spread of fixations (°)*: The standard deviation of the horizontal and vertical gaze angle of fixations.
(v) *Gaze speed ($^\circ/s$)*: The change of the gaze angle over time.
(vi) *Miss rate (%)*: Percentage of undetected visual stimuli.
(vii) *Reaction time (s)*: The elapsed time between the visibility and detection of a visual stimulus.
(viii) *Acceptance Score ($-$)*: A combination of the navigation condition's Usefulness score and Satisfying score.

Calculating gaze angles, fixations, and saccade lengths in VR requires extra attention because participants can freely turn their heads and move through the simulation environment while driving the vehicle. A detailed description of these calculations can be found in Appendix B, below is a brief summary.

1) Gaze angles: The horizontal and vertical gaze angles, θ_h and θ_v, were calculated relative to the vehicles forward unit vector using Equations 1 and 2. Where $\hat{g}$ is the unit vector of participants gaze direction and $\hat{v}$ the forward unit vector of the vehicle.

$$\theta_h = \cos(\hat{g_{xy}} \cdot \hat{v_{xy}})^{-1} \tag{1}$$

$$\theta_v = \cos(\hat{g_{xz}} \cdot \hat{v_{xz}})^{-1} \tag{2}$$

2) Fixations: Fixations were calculated using a dispersion-threshold identification (I-DT) algorithm adjusted for immersive environments, developed by Llanes-Jurado et al. [32]. The I-DT algorithm uses participants' gaze points i.e., the 3D coordinates of the first intersection of participants' gaze direction and a simulated object; coordinates of participants' head position; and a dispersion threshold, θ_{th}. A group of gaze points were marked as a fixation when all angles, θ, met the dispersion threshold, see Equations 3 and 4. Then, the horizontal and vertical gaze angle of the fixation was calculated by averaging the gaze angles of these gaze points.

$$\cos\theta_{ij} = \frac{d_i \cdot d_j}{|d_i|\,|d_j|}, \text{ with } \quad d_n = g_n - \bar{h}_n \tag{3}$$

$$max(\theta) \leq \theta_{th} \tag{4}$$

Where g_n is a subset of gaze points, $\bar{h}_n$ is the average head position over this subset n, and d_n is a list of vectors pointing from the average head position towards the gaze points. The sub-indices i and j are of two arbitrary points within this subset. The subset n is always chronologically ordered.

3) Saccade lengths: Saccade lengths were calculated by summing the differences in angle of gaze vectors between two successive fixations. The gaze vector, v, points from participants head position towards the gaze point. The saccade lengths were calculated using Equations 5 and 6.

$$SL = \sum_{1}^{N} \Delta\theta_i \tag{5}$$

$$\Delta\theta_i = cos(\hat{v}_i \cdot \hat{v}_{i-1})^{-1} \tag{6}$$

Where SL was the saccade length, N was the number of recorded gaze vectors between two successive fixations, and $\Delta\theta_i$ is the angle between two successive gaze vectors.

G. Experimental procedure

Firstly, all participants read and signed the informed consent form and filled in a demographic's questionnaire. Then, they were informed on the practicalities of the experiment i.e., the visual search task, automated acceleration, and the location of detection buttons. Next, they were seated at the simulator, asked to equip the VR headset, and to adjust the seat and headset position to their liking. Then, the built-in eye-tracking calibration of the VR-2 Pro headset was performed, and calibration quality was confirmed to be 'high' (the headset had three calibration quality levels: 'low', 'medium', and 'high').

After calibration, participants drove a 6-minute practice trial to become familiar with the three navigation conditions (each condition was shown for about 2 minutes); the visual stimuli; the vehicle dynamics; and the buttons used for reporting the detection of stimuli. Participants were instructed to drive as they would normally do; to drive in the centre of the road; to follow the navigation instructions; and to report a detection as quickly as possible. After the practice trial, they drove three experimental trials. After each experimental trial, participants

were asked to fill in both the Misery Scale (MISC) [48] and the van der Laan Acceptance Scale. Eye-tracking was re-calibrated before the start of each trial.

Immersive environments can cause participants to become uncomfortable or experience motion sickness. The MISC was used to monitor participants' well-being. It required participants to score their well-being by the following definitions: no problems (0); slight discomfort (1); dizziness, headache, sweating (2,3,4,5); Nausea (6,7,8,9). The experiment was stopped when participants rated their well-being at 6 or higher. All forms and questionnaires used during the experiment can be found in Appendix F.

III. Results

The goal of this study was to measure the effect of conformal compared to non-conformal symbology on drivers' visual search. An effect of symbology type was established when the conformal VC condition differed significantly from both the non-conformal HL and HH conditions while the HH and HL conditions did not significantly differ from each other. Nineteen participants volunteered for this study; however, one participant experienced an uncomfortable level of motion sickness after which the experiment was stopped; their data was discarded. This prompted an analysis of the frame rate which can be seen in the final subsection.

To examine participants' visual search nine objective measures were reported: the miss rate of visual stimuli, the mean reaction time to visual stimuli, the mean fixation duration, the mean fixation rate, the mean saccade length, the horizontal and vertical deviation of the fixation angle, and the mean horizontal and vertical gaze speed. Also, the van der Laan Acceptance Scale was used to measure subjective ratings which is expressed as a Usefulness and Satisfying Score. The means and variation of all measures are shown in Table I. Additionally, to analyse how drivers focused their attention on key objects, an object of interest (OOI) analysis was performed using the mean number of fixations and the mean fixation duration on the OOI. The objects of interest were the visual stimuli used in the visual search task and the navigation symbology. The results of the OOI analysis are shown in Table II. All objective measures, including the OOI, are shown in Figure 7 with the standard deviation shown as the confidence interval. For the interested reader, participants' individual data is shown in Appendix E.

Each measure will be individually analysed in the following subsections. In all analysis, a repeated measures ANOVA was used to test for an initial main effect of navigation conditions and a paired sampled t-test was used for the post-hoc analysis. In cases where Mauchly's test showed that the assumption of sphericity was violated the degrees of freedom were corrected using the Greenhouse-Geisser Epsilon correction. In cases where the Shapiro-Wilk test suggested that the assumption of normality was violated, the Friedman test was used to test for an initial main effect of navigation conditions and Wilcoxon signed-rank test was used as post-hoc analysis. Wilcoxon signed-rank test assumes a normal distribution of

TABLE I: Means and standard deviations of all reported measures, excluding the OOI, averaged across conditions.

Condition:	**HL**	**HH**	**VC**
Visual search task			
Miss rate (%)	44.1 (11)	43.7 (10)	37.7 (11)
Mean reaction time (s)	10.83 (1.61)	11.22 (1.93)	11.13 (2.16)
Eye-measures			
Mean fixation duration (ms)	245 (18.4)	253 (12.7)	255 (17.5)
Mean fixation rate ($\#/s$)	1.14 (0.17)	1.17 (0.11)	1.19 (0.16)
Mean Saccade length (°)	26.80 (9.11)	24.29 (7.10)	22.89 (8.12)
Horizontal spread (°)	13.52 (3.31)	12.63 (2.81)	13.01 (2.72)
Vertical spread (°)	4.91 (1.26)	4.72 (1.03)	4.98 (1.78)
Mean hor. gaze speed (°/s)	48.32 (10.23)	45.51 (11.18)	44.44 (8.30)
Mean ver. gaze speed (°/s)	17.12 (6.32)	15.58 (6.57)	15.69 (6.04)
Subjective measures			
Usefulness score	0.64 (1.03)	0.32 (0.59)	1.16 (0.97)
Satisfying score	0.76 (0.73)	0.56 (0.47)	1.13 (0.75)
Other measures			
Mean driving time (s)	376.2 (13.1)	376.6 (11.9)	373.8 (7.7)
Total navigation errors ($-$)	0	1	1

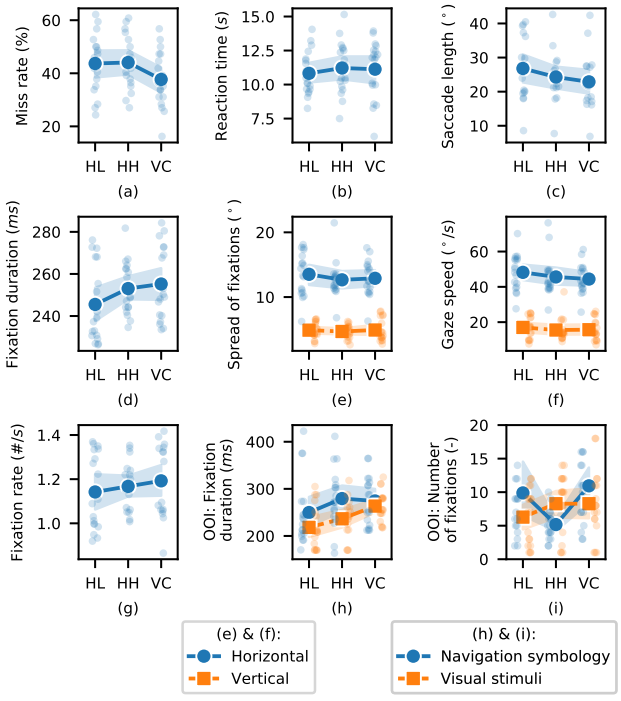

Fig. 6: Histogram of all participants' fixations across condition, with the horizontal and vertical gaze angle on the x-axis and the distance on the y-axis. The size of the histogram bins is 6° and 10 m for the x- and y-axis, respectively.

differences between conditions when this assumption was not met the paired-samples sign test was used instead. Post-hoc test significant levels of $p < 0.05$ were corrected using the Bonferroni correction, resulting in a required significance level of $p < 0.017$.

A. Visual inspection of fixations

Figure 6 shows the distribution fixation locations across conditions, with the horizontal and vertical gaze angles on the x-axis and the distance on the y-axis. The distribution of fixations is near normally distributed with a mean at 0° for all conditions. Some differences can be seen in the vertical fixation angles. The vertical angles of the HH condition were slightly skewed upward compared to the other conditions. This is to be expected as the HH condition had its symbology at a high position. Similar results were not seen for the VC condition which showed a narrower distribution of vertical angles, with a larger portion of fixations around 0°. However, these differences in vertical angles were not reflected by significant differences in the standard deviations seen in Table I.

B. Miss rate

The miss rate of visual stimuli during the visual search task was an indicator of participants' visual search capacity. There was a near significant main effect of navigation conditions ($F(2, 34) = 6.265$, $p = 0.005$). Miss rates were lower while using conformal symbology compared to non-conformal symbology, with an average decrease of 14%.

Miss rates with the VC condition were lower than both the HL ($t(17) = 2.798$, $p = 0.012$) and HH ($t(17) = 2.626$, $p = 0.018$) conditions. While no significant differences between the HH and HL conditions was found ($t(17) = 0.276$, $p = 0.786$). Note, that the VC and HH condition differed with a p-value of 0.018 which was just above the corrected significance level of 0.017.

C. Reaction time

The reaction time during the visual search task was also an indicator of participants' visual search capacity. Even though there were significant differences in miss rates there was no significant main effect of navigation conditions on the reaction time ($F(2, 34) = 0.437$, $p = 0.65$).

D. Fixation duration

The fixation duration was a measure of participants' visual processing time and was calculated as the mean time spent during each fixation. There was significant main effect of navigation conditions ($\chi^2(2) = 8.444$, $p = 0.015$, normality assumption violated $W(18) = 0.860$, $p = 0.012$). However, no significant difference between symbology types was found

E. Fixation rate

The fixation rate was calculated as number of fixation per second and was a measure of participants' sampling rate. There was a significant main effect of navigation conditions ($\chi^2(2) = 7.000$, $p = 0.030$, normality assumption was violated $W(18) = 0.874$, $p = 0.021$). However, no significant differences between symbology types could be established.

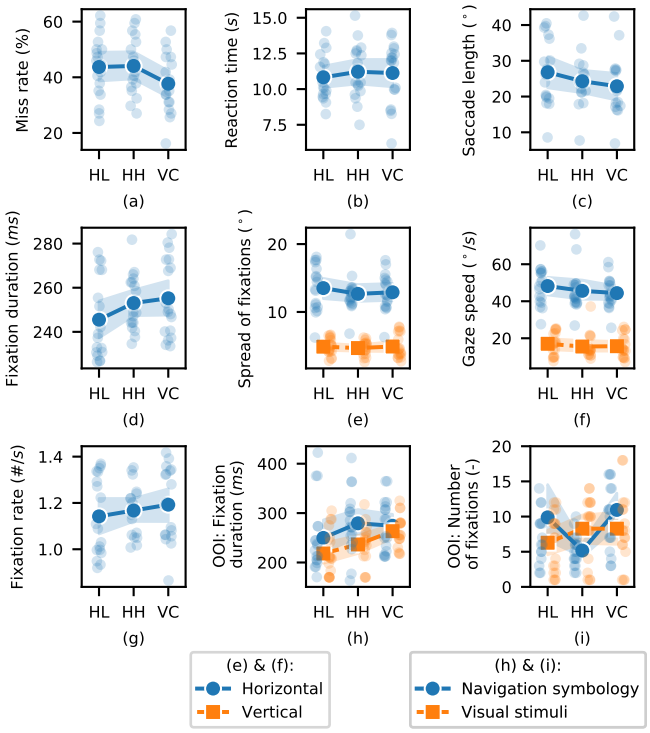

Fig. 7: This figure shows the individual data points, the mean, and the standard deviation (shown by the confidence interval) of all reported measures across navigation conditions: (a) miss rate, (b) reaction time, (c) mean saccade length, (d) mean fixation duration, (e) Spread of fixation angles, (f) gaze speed, (g) fixation rate, (h) mean fixation duration on OOI, and (i) number of fixations on OOI.

F. Saccade length

Mean saccade lengths were calculated as the average angular path traversed between successive fixations. There was a significant main effect of navigation conditions ($F(2, 34) = 3.340$, $p = 0.047$). However, no significant effects of symbology type or position was found. The VC and HL conditions differed significantly ($t(17) = 2.826$, $p = 0.012$), whereas the VC and HH did not ($t(17) = -1.059$, $p = 0.305$).

G. Horizontal and vertical spread

The horizontal and vertical spread was calculated as the standard deviation of fixation's horizontal and vertical gaze angles and was a measure of participants' spread of search. Both measures violated the normality assumption ($W(18) < 0.847, p < 0.007$). No significant main effect of navigation conditions was found for either the horizontal spread ($\chi^2(2) = 0.444$, $p = 0.801$) or the vertical spread ($\chi^2(2) = 0.778$, $p = 0.678$).

TABLE II: Means and standard deviations of the total number of fixations and fixation duration on OOI's across conditions.

Condition:	**HL**		**HH**		**VC**	
Variable:	# Fixations $(-)$	Fixation duration (ms)	# Fixations $(-)$	Fixation duration (ms)	# Fixations $(-)$	Fixation duration (ms)
Visual stimuli	6.28 (4.11)	218 (46)	8.28 (4.53)	236 (40)	8.28 (4.94)	263 (32)
Navigation symbology	11.50 (8.54)	242 (57)	9.78 (5.51)	292 (30)	10.94 (5.71)	274 (52)

H. Horizontal and vertical gaze speed

The horizontal and vertical gaze speeds were calculated as difference in gaze angle over time and were measures of search intensity i.e., how fast participants were directing their gaze over the environment. There was a main effect of navigation conditions for both the horizontal gaze speed ($F(2, 34) = 4.807$, $p = 0.015$) and vertical gaze speed ($\chi^2(2) = 8.444$, $p = 0.015$, normality assumption was violated ($W(18) = 0.844$, $p = 0.007$). However, no significant effects of symbology type were found.

I. Object of interest analysis

The visual stimuli and navigation symbology were the key objects of interest. For both objects of interest, the mean number of fixations and mean fixation duration were reported, see Table II. Most of the data was not normally distributed and thus the Friedman and Wilcoxon signed ranks test were used.

Regarding the navigation symbology, a significant main effect of navigation conditions was found for the mean fixation duration ($\chi^2(2) = 10.111$, $p = 0.006$), but no significant effect for the mean number of fixations was found ($\chi^2(2) = 0.794$, $p = 0.672$). However, no significant differences between symbology type of position were found for the mean fixation duration.

Regarding the visual stimuli, again a significant main effect of navigation conditions was found for the mean fixation duration ($\chi^2(2) = 12.333$, $p = 0.002$), but no significant effect for the mean number of fixations ($\chi^2(2) = 4.030$, $p = 0.133$). Conformal symbology resulted in a significantly higher fixation duration on visual stimuli compared to non-conformal symbology (VC vs. HL: $Z = -3.720, p < 0.001$, VC vs. HH: $Z = -2.288$, $p = 0.022$).

J. Acceptance score

The acceptance score was measured using the van der Laan questionnaire which participants filled in directly after they drove with the corresponding navigation condition. It was a measure of participants' acceptance of the provided navigation condition and consisted of both a usefulness and satisfying score ranging from -2 to +2. The results can be seen in Table I. Both scores showed a significant main effect of navigation conditions ($F(2, 34) < 5.538, p < 0.01$). Participants on average scored the VC as most useful and most satisfying, followed by the HL condition and the HH condition, respectively.

K. Frame rate

The frame rate acquired during the experiment also deserves attention because it is an important factor for participants' VR experience. The mean frame rate across all experimental trials was 50.74 fps with a standard deviation of 11.7. A frame rate of 50 fps is on the low side when considering VR applications (60 fps is generally aimed for), more importantly, the standard deviation is high which is undesirable because changes in frame rate may cause jitter or tearing which increases the risk of motion sickness. Further analysis of the frame rate showed that 21% of the frames fell below 40 fps and 5% below 30 fps. These drops in frame rate are most likely the cause of the uncomfortable level of motion sickness experienced by one of the participants.

The frame drops occurred almost exclusively while participants were performing a turn. Often, a sudden increase in the number of simulated objects is the cause for frame drops. However, it was found that not the number of simulated objects but the rotation of the VR headset within the environment was causing the frame drops. This most likely is due to the underlying implementation of translating the 3D environment to a binocular view as used by the headset.

It is worth noting that the recorded eye-measures were recorded by the built-in VR headset software and not through the simulation software. Therefore, the eye-measures were not affected by the frame rate of the simulation. The eye-tracker had an average measurement frequency of 99.5 Hz across all experimental trials with a standard deviation of 18.0. Where 96.5% of the eye-measures were captured with a frequency higher than 80 Hz.

IV. Discussion

One of the more interesting results were seen in participants' performance in the visual search task. Participants had a close to significant decrease in miss rate ($p = 0.018 > 0.017$) when using conformal symbology compared to non-conformal symbology, on average lowering their miss rates with 14%, from an average of 43.9% to 37.7%. Furthermore, participants rated the conformal symbology as significantly more useful and satisfying which indicated an increased ease of use. This is in line with the results of Boston and Braun [2] who showed that extracting information from the environment was quicker and subjectively rated easier when using conformal symbology compared to non-conformal symbology. Interestingly, the decrease in miss rate was not accompanied by a decrease in reaction time to the visual stimuli. In literature, a decrease in reaction time is often reported when comparing conformal and non-conformal symbology types [2, 12, 16]. It is suspected this discrepancy is due to the nature of the visual search task. The visual search task was designed to stimulate active searching of the environment; stimuli had

low transparencies, α=2/255, resulting in participants regularly missing stimuli which were in their direct line of sight. This level of difficulty may have encouraged participants to adapt their search strategy such that they were more thorough while inspecting the environment, valuing their detection rate over their reaction speed. The object of interest analysis provides additional evidence for this hypothesis. Mean fixation duration on visual stimuli was significantly higher with conformal symbology, with an average increase of 16%, from an average of 227 to 263 ms. This may indicate participants had more time to focus their attention on the visual search task, taking additional time to assess whether a stimulus was present, consequently, decreasing their miss rate.

Performance differences on the visual search task were not supported by significant differences in the reported eye-measures. Nonetheless, there was a notable trend in mean saccade lengths which were lower when participants used conformal symbology. This may indicate that participants made calmer eye-movements which is in line with other studies on conformal navigation systems who obtained similar results [34, 40].

Without significant differences in eye-measures it is hard to explain the observed positive effect on miss rates. It could be argued that the positive effect was due to the conformal symbology being larger than the non-conformal symbology. The conformal symbology covered a much larger vertical visual angle compared to the non-conformal symbology, 42° and 4.1∘, respectively. However, it has been shown that the effect of stimulus size has no effect on participants' reaction time or accuracy for a multitude of tasks, given that the symbology is still readable [23, 25]. The readability of the displays was assessed using the measures obtained from the OOI analysis: the number of fixations and mean fixation duration on the navigation symbology. There were no significant differences between the symbology types thus, it seems unlikely that the non-conformal display was not readable and that the difference in size were the cause of the reported differences between symbology types.

A theoretical explanation can be formulated from the standpoint of an object-based visual attention model. It predicts the benefit of conformal symbology because of the 'fusion' of the symbology with its far domain counterpart such that they become part of the same perceptual group [49]. A perceptual group is often defined as the elements in a visual scene organized by one or more Gestalt grouping principles [5] (e.g., proximity, similarity, symmetry). Several studies showed a positive effect on subjects' accuracy and reaction time when stimuli were presented in the same perceptual group, relative to when the stimuli were in different perceptual groups [5, 9, 10, 18]. Considering the results of the present experiment, the positive effects on miss rates could be explained because the conformal symbology became part of the perceptual group of the environment e.g., the road, whereas the non-conformal symbology became part of the perceptual group of the vehicle. Then, searching for visual stimuli within the environment, while also sampling the navigation instructions, would be easier when using the conformal symbology.

It is difficult to be conclusive on the mechanisms responsible for the reported benefits of conformal symbology. However, the positive effects on participants miss rate is a clear indication that they were more capable of attending the environment while also following the presented navigation instructions while using conformal symbology.

A. Limitation and recommendations

There are a number of limitations and recommendations regarding the present experiment. Firstly, it must be noted that the navigation task was simple e.g., no complex crossings, no other road-users, no traffic lights. A more complex navigation task would be preferred as this may increase the potential advantages of more intuitive navigation instructions and therefore, show more conclusive results. Secondly, the difficulty of the visual search task was not calibrated for individually each participant causing discrepancies in the task difficulty. Calibration of the visual search task's difficulty is recommended in order to equalise the workload. Lastly, the non-conformal symbology had a simple format, deviating from the standard symbology used in today's personal navigation devices e.g., Google Maps. This simple format may have been less intuitive, requiring increased effort in reading the instructions. Non-conformal symbology resembling today's standards should be preferred, especially when also incorporating more complex navigation tasks.

Additional aspects to consider are that driver behaviour may have differed within this simulation because there were no risks of physical accidents, no other road-users were present, and the vehicles acceleration was automated. Also, the simulation exhibited relatively low frame rate; averaging at 50 fps but regularly dropping below 40 fps when participants drove a turn. The low frame rate was caused by the rotation of the VR headset within the simulated environment e.g., during a turn. How to prevent such drops in frame rate during turns is still unclear but further development of this VR driving simulator should focus on addressing this issue.

V. Conclusion

The current findings provide additional evidence supporting the benefits of conformal symbology. Visual search skill of drivers was improved, significantly decreasing miss rates during the visual search task with 14%, from 44% to 38%. Additionally, participants had an increased mean fixation duration on visual stimuli of 16%, from 227 ms to 263 ms. Furthermore, subjective ratings indicated that the conformal symbology was preferred over the non-conformal symbology.

Findings concerning the reported eye-measures were less clear. Eye-movements when using conformal symbology had a trend to be calmer with lower mean saccade lengths. Although these differences were not statistically significant, they were an indication of calmer gazing behaviour. Similar results have been established in comparable studies.

For future research it is recommended to increase the complexity of the primary driving task e.g., by adding other road

users, roundabouts, and more complex intersections. A more complex driving task will most likely increase the observed differences providing more support for the benefit of conformal symbology. Also, it's advised to calibrate the difficulty of the visual search task individually for each participant in order to equalise the workload of all participants. Additionally, it is recommended to redesign the non-conformal symbology to resemble today's standards more closely. Furthermore, before using this VR driving simulator, the technical issues which occur while participants drove a turn requires attention.

REFERENCES

[1] P. Bazilinskyy, L. Kooijman, D. Dodou, and J. de Winter. Coupled simulator for research on the interaction between pedestrians and (automated) vehicles. Sept. 2020. 00002.

[2] B. N. Boston and C. C. Braun. Clutter and Display Conformality: Changes in Cognitive Capture, 1996. 00011.

[3] P. Chapman, G. Underwood, and K. Roberts. Visual search patterns in trained and untrained novice drivers. *Transportation Research Part F: Traffic Psychology and Behaviour*, 5(2):157–167, June 2002. ISSN 1369-8478. doi: 10.1016/S1369-8478(02)00014-1. URL https://www.sciencedirect.com/science/article/pii/S1369847802000141. 00287.

[4] P. R. Chapman and G. Underwood. Visual Search of Driving Situations: Danger and Experience. *Perception*, 27(8):951–964, Aug. 1998. ISSN 0301-0066. doi: 10.1068/p270951. URL https://doi.org/10.1068/p270951. 00470 Publisher: SAGE Publications Ltd STM.

[5] Z. Chen. Object-based attention: A tutorial review. *Attention, Perception, & Psychophysics*, 74(5):784–802, July 2012. ISSN 1943-393X. doi: 10.3758/s13414-012-0322-z. URL https://doi.org/10.3758/s13414-012-0322-z. 00170.

[6] V. Clay, P. König, and S. König. Eye Tracking in Virtual Reality. *Journal of Eye Movement Research*, 12(1):10.16910/jemr.12.1.3, 2019. ISSN 1995-8692. doi: 10.16910/jemr.12.1.3. URL https://www.ncbi.nlm.nih.gov/pmc/articles/PMC7903250/. 00058.

[7] A. T. Duchowski, V. Shivashankaraiah, T. Rawls, A. K. Gramopadhye, B. J. Melloy, and B. Kanki. Binocular eye tracking in virtual reality for inspection training. In *Proceedings of the 2000 symposium on Eye tracking research & applications*, ETRA '00, pages 89–96, New York, NY, USA, Nov. 2000. Association for Computing Machinery. ISBN 978-1-58113-280-9. doi: 10.1145/355017.355031. URL https://doi.org/10.1145/355017.355031. 00113.

[8] T. Dukic and T. Broberg. Older drivers' visual search behaviour at intersections. *Transportation Research Part F: Traffic Psychology and Behaviour*, 15(4):462–470, July 2012. ISSN 1369-8478. doi: 10.1016/j.trf.2011.10.001. URL https://www.sciencedirect.com/science/article/pii/S1369847811000994. 00080.

[9] J. Duncan. Selective attention and the organization of visual information. *Journal of Experimental Psychology: General*, 113(4):501–517, 1984. ISSN 1939-2222(Electronic),0096-3445(Print). doi: 10.1037/0096-3445.113.4.501. 02603 Place: US Publisher: American Psychological Association.

[10] R. Egly, J. Driver, and R. D. Rafal. Shifting visual attention between objects and locations: Evidence from normal and parietal lesion subjects. *Journal of Experimental Psychology: General*, 123(2):161–177, 1994. ISSN 1939-2222(Electronic),0096-3445(Print). doi: 10.1037/0096-3445.123.2.161. 01438 Place: US Publisher: American Psychological Association.

[11] R. Eyraud, E. Zibetti, and T. Baccino. Allocation of visual attention while driving with simulated augmented reality. *Transportation Research Part F: Traffic Psychology and Behaviour*, 32:46–55, July 2015. ISSN 1369-8478. doi: 10.1016/j.trf.2015.04.011. URL https://www.sciencedirect.com/science/article/pii/S1369847815000741. 00032.

[12] S. Fadden, P. M. Ververs, and C. D. Wickens. Costs and Benefits of Head-Up Display Use: A Meta-Analytic Approach. *Proceedings of the Human Factors and Ergonomics Society Annual Meeting*, 42(1):16–20, Oct. 1998. ISSN 2169-5067. doi: 10.1177/154193129804200105. URL https://doi.org/10.1177/154193129804200105. 00099.

[13] N. d. O. Faria, J. L. Gabbard, and M. Smith. Place in the World or Place on the Screen? Investigating the Effects of Augmented Reality Head -Up Display User Interfaces on Drivers' Spatial Knowledge Acquisition and Glance Behavior. In *2020 IEEE Conference on Virtual Reality and 3D User Interfaces Abstracts and Workshops (VRW)*, pages 762–763, Mar. 2020. doi: 10.1109/VRW50115.2020.00232. 00000.

[14] J. L. Gabbard. Behind the Glass: Driver Challenges and Opportunities for AR Automotive Applications - IEEE Journals & Magazine, 2013. 00000.

[15] J. L. Gabbard, M. Smith, K. Tanous, H. Kim, and B. Jonas. AR DriveSim: An Immersive Driving Simulator for Augmented Reality Head-Up Display Research. *Frontiers in Robotics and AI*, 0, 2019. ISSN 2296-9144. doi: 10.3389/frobt.2019.00098. URL https://internal-journal.frontiersin.org/articles/10.3389/frobt.2019.00098/full. 00006 Publisher: Frontiers.

[16] K. W. Gish and L. Staplin. Human factors aspects of using head up displays in automobiles: a review of the literature. interim report. 1995. doi: 10.1037/e509202009-001. 00000.

[17] L. Hagen. *The use of head-up displays (HUDS) in motor vehicles*. Master of Arts, Carleton University, Ottawa, Ontario, 2005. URL https://curve.carleton.ca/9ea0f519-3d3a-420c-9e0c-6d0def0faaf7. 00000.

[18] S. Han and G. W. Humphreys. Interactions between perceptual organization based on Gestalt laws and those based on hierarchical processing. *Perception & Psychophysics*, 61(7):1287–1298, Jan. 1999. ISSN 0031-

5117, 1532-5962. doi: 10.3758/BF03206180. URL http://link.springer.com/10.3758/BF03206180. 00092.

[19] G. Ho, C. T. Scialfa, J. K. Caird, and T. Graw. Visual Search for Traffic Signs: The Effects of Clutter, Luminance, and Aging. *Human Factors*, 43(2):194–207, June 2001. ISSN 0018-7208. doi: 10.1518/001872001775900922. URL https://doi.org/10.1518/001872001775900922. 00205 Publisher: SAGE Publications Inc.

[20] M. Homan. The use of optical waveguides in Head Up Display (HUD) applications. volume 8736, page 87360E, June 2013. doi: 10.1117/12.2014513. 00029.

[21] W. J. Horrey, A. L. Alexander, and C. D. Wickens. Does workload modulate the effects of in-vehicle display location on concurrent driving and side task performance. In *Driving Simulation Conference North America, Dearborn, Michigan*, pages 1–20, 2003. 00027.

[22] Y. Inuzuka, Y. Osumi, and H. Shinkai. Visibility of Head up Display (HUD) for Automobiles. *Proceedings of the Human Factors Society Annual Meeting*, 35 (20):1574–1578, Sept. 1991. ISSN 0163-5182. doi: 10.1177/154193129103502033. URL https://doi.org/10.1177/154193129103502033. 00053 Publisher: SAGE Publications.

[23] J. T. Q. Jr, R. A. Schmidt, H. N. Zelaznik, B. Hawkins, and R. McFarquhar. Target-Size Influences on Reaction Time with Movement Time Controlled. *Journal of Motor Behavior*, 12(4):239–261, Dec. 1980. ISSN 0022-2895. doi: 10.1080/00222895.1980.10735224. URL https://doi.org/10.1080/00222895.1980.10735224. 00055 Publisher: Routledge _eprint: https://doi.org/10.1080/00222895.1980.10735224.

[24] A. Kahana. Obstacle-Avoidance Displays for Helicopter Operations: Spatial Versus Guidance Symbologies. *Journal of Aerospace Information Systems*, 12(7): 455–466, 2015. doi: 10.2514/1.I010306. URL https://doi.org/10.2514/1.I010306. 00000 Publisher: American Institute of Aeronautics and Astronautics _eprint: https://doi.org/10.2514/1.I010306.

[25] W. N. Kama and G. G. Kuperman. The Effect of HUD (Head-Up-Display) Symbology Size on Operator Performance Under Various Luminance Conditions. Technical report, HARRY G ARMSTRONG AEROSPACE MEDICAL RESEARCH LAB WRIGHT-PATTERSON AFB OH, Dec. 1987. URL https://apps.dtic.mil/sti/citations/ADA210460. 00000 Section: Technical Reports.

[26] R. J. Kiefer and A. W. Gellatly. Quantifying the Consequences of the "Eyes-on-Road" Benefit Attributed to Head-Up Displays. *SAE Transactions*, 105:1219–1240, 1996. ISSN 0096-736X. URL https://www.jstor.org/stable/44720840. 00020 Publisher: SAE International.

[27] P. Konstantopoulos, P. Chapman, and D. Crundall. Exploring the ability to identify visual search differences when observing drivers' eye movements. *Transportation Research Part F: Traffic Psychology and Behaviour*, 15 (3):378–386, May 2012. ISSN 1369-8478. doi: 10.1016/j.trf.2011.02.005. URL https://www.sciencedirect.com/science/article/pii/S1369847811000763. 00029.

[28] C. T. J. Lamers and J. G. Ramaekers. Visual search and urban driving under the influence of marijuana and alcohol. *Human Psychopharmacology: Clinical and Experimental*, 16(5):393–401, 2001. ISSN 1099-1077. doi: 10.1002/hup.307. URL https://onlinelibrary.wiley.com/doi/abs/10.1002/hup.307. 00118 _eprint: https://onlinelibrary.wiley.com/doi/pdf/10.1002/hup.307.

[29] H. C. Lee, A. H. Lee, and D. Cameron. Validation of a Driving Simulator by Measuring the Visual Attention Skill of Older Adult Drivers. *American Journal of Occupational Therapy*, 57(3):324–328, May 2003. ISSN 0272-9490. doi: 10.5014/ajot.57.3.324. URL https://ajot.aota.org/article.aspx?articleid=1869381. 00099 Publisher: American Occupational Therapy Association.

[30] J.-h. Lee, I. Yanusik, Y. Choi, B. Kang, C. Hwang, J. Park, D. Nam, and S. Hong. Automotive augmented reality 3D head-up display based on light-field rendering with eye-tracking. *Optics Express*, 28(20):29788–29804, Sept. 2020. ISSN 1094-4087. doi: 10.1364/OE.404318. URL https://www.osapublishing.org/oe/abstract.cfm?uri=oe-28-20-29788. 00005 Publisher: Optical Society of America.

[31] S. C. Lee, Y. W. Kim, and Y. G. Ji. Effects of visual complexity of in-vehicle information display: Age-related differences in visual search task in the driving context. *Applied Ergonomics*, 81:102888, Nov. 2019. ISSN 0003-6870. doi: 10.1016/j.apergo.2019.102888. URL https://www.sciencedirect.com/science/article/pii/S0003687019301206. 00011.

[32] J. Llanes-Jurado, J. Marín-Morales, J. Guixeres, and M. Alcañiz. Development and Calibration of an Eye-Tracking Fixation Identification Algorithm for Immersive Virtual Reality. *Sensors*, 20(17):4956, Jan. 2020. doi: 10.3390/s20174956. URL https://www.mdpi.com/1424-8220/20/17/4956. 00004 Number: 17 Publisher: Multidisciplinary Digital Publishing Institute.

[33] R. Martin-Emerson and C. D. Wickens. Superimposition, Symbology, Visual Attention, and the Head-Up Display. *Human Factors*, 39(4):581–601, Dec. 1997. ISSN 0018-7208. doi: 10.1518/001872097778667933. URL https://doi.org/10.1518/001872097778667933. 00101.

[34] Z. Medenica, A. L. Kun, T. Paek, and O. Palinko. Augmented reality vs. street views: a driving simulator study comparing two emerging navigation aids. In *Proceedings of the 13th International Conference on Human Computer Interaction with Mobile Devices and Services*, MobileHCI '11, pages 265–274, Stockholm, Sweden, Aug. 2011. Association for Computing Machinery. ISBN 978-1-4503-0541-9. doi: 10.1145/2037373.2037414. URL https://doi.org/10.1145/2037373.2037414. 00106.

[35] C. Merenda, C. Suga, J. L. Gabbard, and T. Misu. Effects of "Real-World" Visual Fidelity on AR Interface Assessment: A Case Study Using AR Head-up Display Graphics in Driving. In *2019 IEEE International Sympo-*

sium on Mixed and Augmented Reality (ISMAR), pages 145–156, Oct. 2019. doi: 10.1109/ISMAR.2019.00-10. 00000 ISSN: 1554-7868.

[36] W. Narzt, G. Pomberger, A. Ferscha, D. Kolb, R. Müller, J. Wieghardt, H. Hörtner, and C. Lindinger. Augmented reality navigation systems. *Universal Access in the Information Society*, 4(3):177–187, Mar. 2006. ISSN 1615-5297. doi: 10.1007/s10209-005-0017-5. URL https://doi.org/10.1007/s10209-005-0017-5. 00000.

[37] T. Poitschke, M. Ablassmeier, G. Rigoll, S. Bardins, S. Kohlbecher, and E. Schneider. Contact-analog information representation in an automotive head-up display. In *Proceedings of the 2008 symposium on Eye tracking research & applications*, ETRA '08, pages 119–122, Savannah, Georgia, Mar. 2008. Association for Computing Machinery. ISBN 978-1-59593-982-1. doi: 10.1145/1344471.1344502. URL https://doi.org/10.1145/1344471.1344502. 00033.

[38] B. Reimer, L. A. D'Ambrosio, J. F. Coughlin, M. E. Kafrissen, and J. Biederman. Using self-reported data to assess the validity of driving simulation data. *Behavior Research Methods*, 38(2):314–324, May 2006. ISSN 1554-3528. doi: 10.3758/BF03192783. URL https://doi.org/10.3758/BF03192783. 00151.

[39] G. H. Robinson, D. J. Erickson, G. L. Thurston, and R. L. Clark. Visual Search by Automobile Drivers. *Human Factors*, 14(4):315–323, Aug. 1972. ISSN 0018-7208. doi: 10.1177/001872087201400404. URL https://doi.org/10.1177/001872087201400404. 00125 Publisher: SAGE Publications Inc.

[40] K. SeungJun and D. Anind K. Simulated augmented reality windshield display as a cognitive mapping aid for elder driver navigation | Proceedings of the SIGCHI Conference on Human Factors in Computing Systems, Apr. 2009. 00000.

[41] D. R. Tufano. Automotive HUDs: The Overlooked Safety Issues, 1997. URL https://journals.sagepub.com/doi/abs/10.1518/001872097778543840. 00153.

[42] E. Y. Uc, M. Rizzo, S. W. Anderson, J. Sparks, R. L. Rodnitzky, and J. D. Dawson. Impaired visual search in drivers with Parkinson's disease. *Annals of Neurology*, 60(4):407–413, 2006. ISSN 1531-8249. doi: 10.1002/ana.20958. URL https://onlinelibrary.wiley.com/doi/abs/10.1002/ana.20958. 00172 _eprint: https://onlinelibrary.wiley.com/doi/pdf/10.1002/ana.20958.

[43] G. Underwood, P. Chapman, K. Bowden, and D. Crundall. Visual search while driving: skill and awareness during inspection of the scene. *Transportation Research Part F: Traffic Psychology and Behaviour*, 5(2):87–97, June 2002. ISSN 1369-8478. doi: 10.1016/S1369-8478(02)00008-6. URL http://www.sciencedirect.com/science/article/pii/S1369847802000086. 00353.

[44] G. Underwood, P. Chapman, N. Brocklehurst, J. Underwood, and D. Crundall. Visual attention while driving: sequences of eye fixations made by experienced and novice drivers. *Ergonomics*, 46(6):629–646, Jan. 2003. ISSN 0014-0139. doi: 10.1080/0014013031000090116. URL https://doi.org/10.1080/0014013031000090116. 00542 Publisher: Taylor & Francis _eprint: https://doi.org/10.1080/0014013031000090116.

[45] J. D. Van Der Laan, A. Heino, and D. De Waard. A simple procedure for the assessment of acceptance of advanced transport telematics. *Transportation Research Part C: Emerging Technologies*, 5(1):1–10, Feb. 1997. ISSN 0968-090X. doi: 10.1016/S0968-090X(96)00025-3. URL https://www.sciencedirect.com/science/article/pii/S0968090X96000253. 00731.

[46] P. M. van Leeuwen, R. Happee, and J. C. F. d. Winter. Investigating the Effect of a Visual Search Task for Simulator-Based Driver Training. *Driving Assessment Conference*, 7:425–431, June 2013. URL https://ir.uiowa.edu/drivingassessment/2013/papers/65. 00005.

[47] P. Ververs and C. D. Wickens. Conformal flight path symbology for head-up displays: Defining the distribution of visual attention in three-dimensional space. 1998. 00000.

[48] A. H. Wertheim, J. E. Bos, and A. J. Krul. *Predicting motion induced vomiting from subjective misery (MISC) ratings obtained in 12 experimental studies*. TNO Human Factors, 2001. 00006.

[49] C. D. Wickens and J. Long. Conformal Symbology, Attention Shifts, and the Head-Up Display. *Proceedings of the Human Factors and Ergonomics Society Annual Meeting*, 38(1):6–10, Oct. 1994. ISSN 2169-5067. doi: 10.1177/154193129403800103. URL https://doi.org/10.1177/154193129403800103. 00000.

[50] J. M. Wolfe and T. S. Horowitz. What attributes guide the deployment of visual attention and how do they do it? *Nature Reviews Neuroscience*, 5(6):495–501, June 2004. ISSN 1471-003X, 1471-0048. doi: 10.1038/nrn1411. URL http://www.nature.com/articles/nrn1411. 00000.

APPENDIX A
VISUAL STIMULI CALIBRATION

***Abstract*—Using visual stimuli in an active visual search task requires a certain level of task difficulty. This experiment was conducted to estimate the radius and transparency of visual stimuli for a visual search task such that the miss rates approach 50%. Six participants drove 15 trials in a Virtual Reality (VR) driving simulator, each trial consisted of two drives in a straight line of 180 m. Visual stimuli were positioned within the environment with varying radii and transparencies per trial. The findings suggest that the radius of the visual stimulus does significantly effect participants' miss rate. Transparency of the visual stimulus did have a significant effect on participants' miss rate. Interpolation of results suggest a transparency of 2 to best approach the desired miss rate of 50%, with an estimated miss rate of 43%.**

A. Introduction

Estimating drivers' visual search can be performed using eye-measurements but also by their performance on a visual search task, requiring detection of visual stimuli [17, 29, 46]. In order to observe the effects of different conditions on the miss rate of visual stimuli it is desirable to have a mean miss rate of 50% for maximum sensitivity e.g., if all participants acquire a miss rate of 0% for all conditions then no information can extracted. Miss rate of stimuli is highly depended on participants' workload, environment and visual attributes of the stimuli [50]. Therefore, it is required to perform some type of calibration of visual stimuli attributes within the specific context in which the stimuli would be shown.

The present study was performed to estimate the transparency and radius of a visual stimulus such that the average miss rate approaches 50% when using the stimulus for a visual search task within the VR driving simulator described in Appendix D.

B. Method

1) Participants: Six participants (all men) volunteered to participate in the experiment. All participants were from the Technical University of Delft and ranged in age from 22 to 29.

2) Apparatus and stimuli: The experiment was conducted using a virtual environment made with game engine Unity version 2019.4.3f1, see Appendix D for a detailed description. The virtual environment consisted of a straight road of 180 meters with pavement, buildings, and other miscellaneous object on the side of the road.

The environment was presented to participants using the Varjo VR-2-Pro, a high-resolution virtual reality glass, equipped with two 1920 x 1080 low persistence micro-OLEDs, two 1440 x 1600 low persistence AMOLEDs, and 90 Hz 20/20 eye tracking. A Logitech G27 steering wheel was used for controlling the vehicle and for responding to the visual stimuli. The visual stimuli used were yellow, semi-transparent spheres with variable transparency, α, and radius, r.

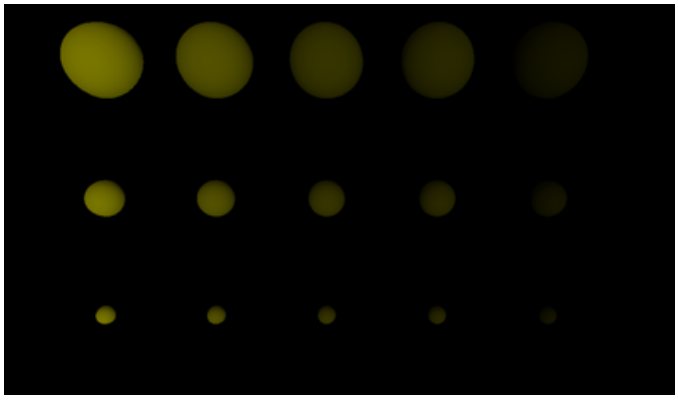

Fig. 8: The 15 combinations of radii (1, 0.75, and 0.5 m) and transparencies (25, 13, 5, 3, and 1) used for the visual stimuli.

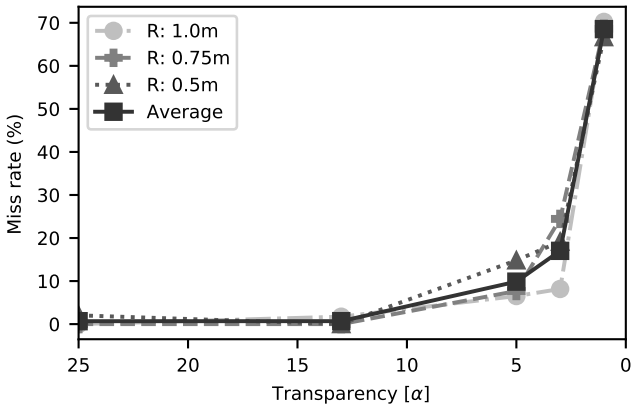

Fig. 9: Miss rate grouped by transparency and radius of visual stimuli.

3) Design and procedure: The transparency, α, and radius, r, were varied incrementally throughout the experiment. The values for α and r were $[25, 13, 5, 3, 1]$ and $[1m, 0.75m, 0.5m]$, respectively. Giving rise to a total of 15 different conditions: C1 being $[r = 1, \alpha = 25]$, C2: $[r = 1, \alpha = 13]$, ..., C15: $[r = .5, \alpha = 1]$. Each condition referring to a combination of visual stimuli attributes, the resultant combinations are shown in Figure 8.

Each participant drove 15 trials, one for each condition, in the following order: C1, C2, ..., C15. Each trial contained a total of 8 visual stimuli and consisted of 2 consecutive drives over the 180 m track. To reduce participants' ability to predict the positions of the visual stimuli, both the number of stimuli and their positions were varied per drive. A minimum of 2 and maximum of 6 stimuli were visible per drive, but this number was constrained such that the two drives for a single condition always contained exactly 8 stimuli.

Detection of visual stimuli were reported using a button on the steering wheel. However, multiple visual stimuli would often be within the field of view of participants. Gaze vectors i.e., origin and direction of participants' gaze, were available

TABLE III: Mean and variation of the miss rate per transparency α.

α	25	13	5	3	1
Miss rate (%)	0.8 (3.4)	0.6 (2.3)	9 (12)	18 (24)	68 (24)

to the simulation environment on a frame-by-frame basis. This information was used to determine which stimuli was being detected at the time of a button press. When a detection was reported, a stimulus was marked as detected if: (1) the gaze vector pointed directly at the stimuli during this frame; or (2) it was the most recently looked at stimuli within half a second of the current frame. After a stimulus was marked as detected it would disappear from the environment functioning as feedback for participants.

Acceleration of the simulated vehicle was automated i.e., participants were only able to steer the vehicle in order to equalise participants' exposure time to the visual stimuli. To keep engagement and realism as high as possible, participants were able to steer the vehicle. If participants hit the curb or any other simulated object during a drive, the vehicle was stopped, and the current drive was performed again.

Participants were given two tasks: (1) keep the car centred on the road, and (2) use the response buttons on the back of the steering wheel to report the detection of a visual stimuli. Before the start of the experiment the participants drove a practise trial to get familiar with the VR headset; the vehicle dynamics e.g., the automated acceleration; and the steering wheel buttons used for reporting a detection. Participants were also informed on the different conditions and their order i.e., that the changing transparency α and radius r would be presented in an increasing level of difficulty and that stimuli during each trial would have the same properties.

C. Results

Statistical analysis was performed using a one-way ANOVA. The radius of the visual stimuli did not have a significant effect on the miss rate ($F(2, 87) = 0.12, p = 0.88$), whereas the transparency did have a significant effect on the miss rate ($F(2, 87) = 53.72, p = 1.7e - 22$). The mean miss rates and their variation are shown in Table III

D. Discussion and conclusion

The miss rates correlated well with the transparency but did not seem affected by the radius of the stimulus. Because RGBA values are required to be integer values between 0 and 255 the choice is limited. An α value of 3 resulted in a mean miss rate of 18%, far below of what is desired. Whereas an α level of 1 resulted in a mean miss rate of 68%, far above the desired miss rate of 50%. Interpolating between the results predicts a mean miss rate of 43% for an α value of 2. An α of 2 would best approach the desired miss rate when used within this VR driving simulator.

It must be noted that searching for visual stimuli was the only task of participants during this experiment. Miss rates would most likely increase when requiring participants to perform additional tasks e.g., watch for other road-users, navigate the vehicle.

APPENDIX B
EYE-MEASURE CALCULATIONS

In this section the calculations of the gaze angles, fixations, and saccade lengths are explained in more detail. The algorithm determining fixations was introduced by Llanes-Jurado et al. [32]; the algorithm was implemented independently and can be found on this[1] GitHub page. Before going into detail on the calculations, a few notes should be made:

1) *The reference frame*: Within the Unity the reference frame is defined such that the z-axis points forward, x-axis points sideways, and y-axis points upwards.
2) *Gaze direction*: An object containing a unit vector indicating the direction of participants' gaze in world-fixed coordinates, and a log time.
3) *Gaze point*: An object containing 3D coordinates in the world-fixed reference frame, a distance, and a log time. The 3d coordinates corresponded to the first intersection with a simulated object when drawing a line from the current position of participants' HMD in the *gaze direction*. The distance was the length of this line. When no objects were hit e.g., participant looking at the sky, a line length of 200 m was used, and the corresponding coordinates calculated. 200 m was approximately the maximum distance that participants had towards any visibly object during the simulation.
4) *Gaze vector*: An object containing a 3D vector pointing from participants HMD position to the gaze point in the world-fixed reference frame and a log time
5) *Gaze angle*: Consisted of both a horizontal and vertical component; calculation shown in section B.
6) *Fixation*: Consisted of a horizontal and vertical gaze angle, a distance, and a duration; calculations shown in section B.
7) *Saccade length*: Consisted of a single value representing the length of the travelled path in °; calculations shown in section B.

A. Gaze angles

Participants were able to move their heads in addition to moving through the VR environment e.g., driving a vehicle. Therefore, a steady frame of reference has to be chosen from which angles can be measured. The simulated vehicle was used as the reference frame as its relative position to the participant did not change unless the participant moved their head e.g., if the vehicle rotated left, participants rotated left as well. This does introduce a minor discrepancy in the particular situation where participants would not rotate their head along with the vehicle during a turn e.g., while focusing on a specific object; this would show as an increase in horizontal gaze angle while in reality their gaze is unchanged. This must be kept in mind while analysing and looking at the horizontal gaze data. The horizontal and vertical gaze angles, θ_h and θ_v, were calculated relative to the vehicles forward unit vector with Equations 1 and 2.

[1]https://github.com/MarcSchotman/thesis

$$\theta_h = \cos(\hat{g_{xy}} \cdot \hat{v_{xy}})^{-1} \tag{7}$$

$$\theta_v = \cos(\hat{g_{xz}} \cdot \hat{v_{xz}})^{-1} \tag{8}$$

Where $\hat{g}$ is participants gaze direction and $\hat{v}$ the unit vector of the forward vector of the vehicle. See Figure 10 for an illustration.

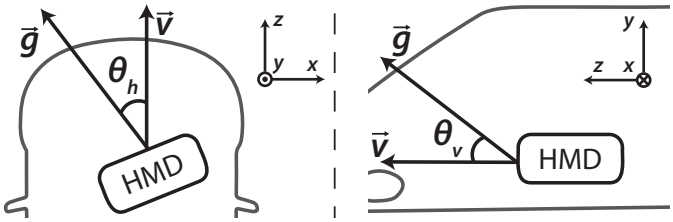

Fig. 10: Definition of the horizontal and vertical gaze angle, θ_h and θv. Here g is the gaze direction vector, and $\vec{v}$ is the forward vector of the vehicle.

B. Fixations

The fixations were determined using a dispersion threshold identification (I-DT) algorithm, adjusted for immersive environments, and developed by Llanes-Jurado et al. [32]. The I-DT algorithm has 5 inputs, the gaze point coordinates; the coordinates of participants' head position; a frequency threshold; time threshold; and a dispersion threshold. The frequency, time, and dispersion thresholds were set at the recommended values by Llanes-Jurado et al. [32] at 30 Hz, 150 ms, and 1°, respectively.

The pseudo code of the algorithm is shown in Algorithm 1. Fixations are found iteratively by starting with the first and smallest subset of head positions and gaze points which meet both the minimum sampling frequency and fixation duration. Then, if the dispersion threshold is not met, see Equations 9 and 10, the last point is marked as a saccade, dropped from the subset, and the next point is added. If all thresholds are met, the subset size is increased until one of the thresholds is broken, then all points in this subset are marked as a single fixation. This process is repeated until all points are marked as either a saccade or fixation. Then, subsequent gaze points which are marked as a fixation are grouped and recorded as a single fixations. Finally, this subset of gaze points was used to calculate the fixations' horizontal gaze angle, vertical gaze angle, distance, and duration. The horizontal gaze angle, vertical gaze angle and distance were calculated by taking the mean of the corresponding values of the subset of gaze points and the duration was calculated by the difference in log time of the first and last gaze point in the set. In Figure 12 two examples of marked gaze points can be seen with fixations in red and saccades in black.

$$\cos\theta_{ij} = \frac{d_i \cdot d_j}{|d_i|\,|d_j|}, \text{ with } \quad d_n = g_n - \bar{h}_n \tag{9}$$

$$max(\theta) \leq \theta_{th} \tag{10}$$

Where d_n is a list of vectors pointing from the average head position towards the gaze points, g_n is a subset of gaze points, and $\bar{h_n}$ is participants' average head position of this subset n. The sub-indices i and j are of two arbitrary points within this subset. A dispersion threshold is met when all angles, θ, are below the dispersion threshold θ_{th}.

C. Saccade length

The goal of measuring saccade lengths was to provide a measure for spread of search. Therefore, the saccade lengths were calculated by estimating the travelled path of the gaze; summing the relative angles between successive gaze vectors between two fixations, see Figure 11. A higher measurement frequency results in a better estimate of the actual travelled path. In Figure 12 some larger jumps between gaze points can be observed which was not ideal. Nonetheless, this measure gives a better indication of the travelled path than simply calculating the angle between two fixation points as illustrated by Figure 11, where the relative angle is much smaller than the travelled path. The saccade lengths were calculated using Equations 11 and 12.

$$SL = \sum_{1}^{N} \Delta\theta_i \tag{11}$$

$$\Delta\theta_i = cos(\hat{v}_i \cdot \hat{v}_{i-1})^{-1} \tag{12}$$

Where SL was the saccade length, N was the number of recorded gaze vectors between two successive fixations, and $\Delta\theta_i$ is the angle between two successive gaze vectors.

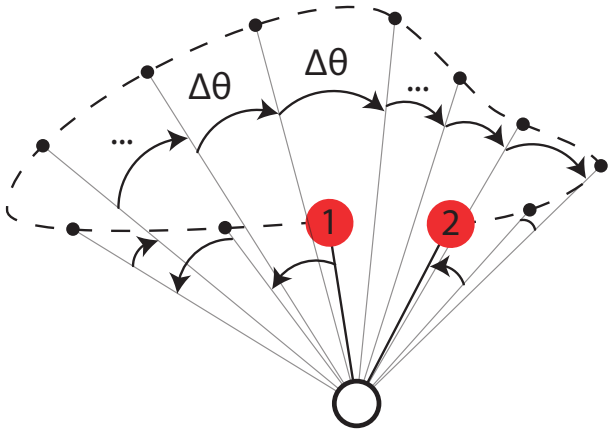

Fig. 11: Illustration of saccade length calculation where the participant is represented by the black circle, fixations by the red circles, and gaze points by the black dots.

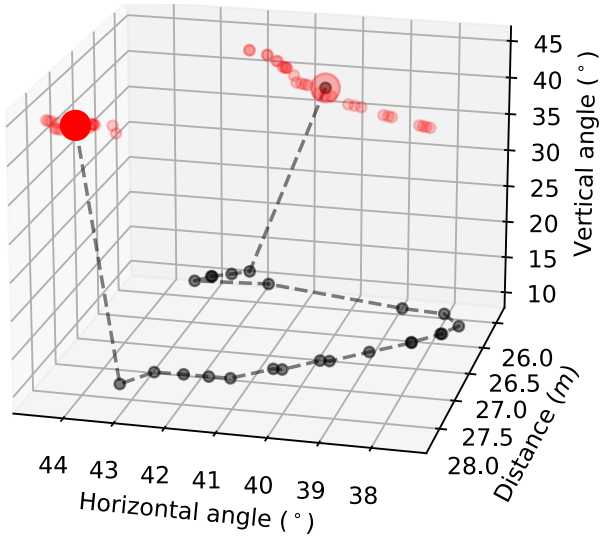

(a)

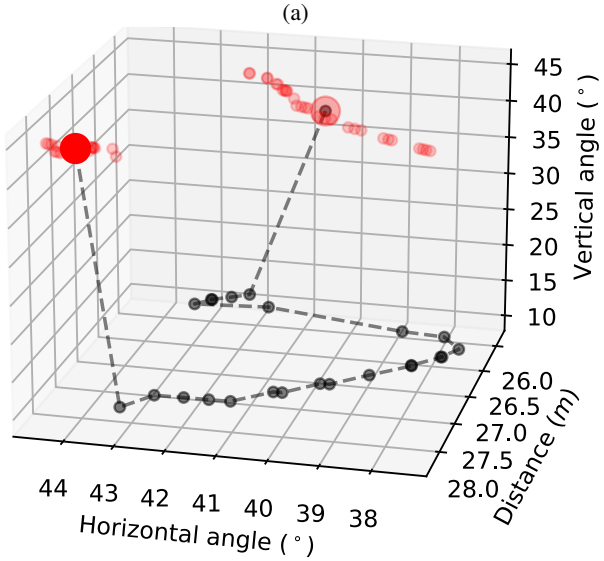

(b)

Fig. 12: Examples of gaze points identified as fixations or saccades. Fixations are marked red and saccades in black. The larger red marker corresponds to the mean gaze angles and distance of the set of marked gaze points, this horizontal angle, vertical angle, and distance were assigned to the specific fixation.

Algorithm 1: Pseudo code of the dispersion-threshold identification protocol from Llanes-Jurado et al. [32]

Input : Frequency threshold (f_{th}), time threshold (t_{th}), dispersion threshold (θ_{th}), list of gaze point positions (g), list of head positions (h), list of log times (t_c)

Output: Boolean list of fixations

```
/* Main I-DT algorithm which loops over all gaze points                    */
Function DT-I(f_th, t_th, θ_th, g, h, t_c):
    Initialise list of indices I
    while indices in I do
        Get list of indices, I_w, complying to t_th
        I_w, success = Thresholds(I_w)
        if success then
            Classify I_w as fixations
            Remove indices I_w from I
        end
        else
            Remove first index of I_w from I
        end
    end
/* Recursive threshold check while increasing window size                  */
Function Thresholds(I_w, success=False):
    Get points, t_w, g_w, h_w, in window I_w
    Compute frequencies, f, of t_w
    Compute angles, θ = Angles(g_w, h_w)
    if max(θ)≤ θ_th and min(f) ≥ f_th then
        Add next index to I_w
        return Thresholds(I_w, True)
    end
    else
        return I_w, success
    end
/* Compute θ for all combinations of gaze vectors                          */
Function Angles(g_w, h_w):
    Compute gaze vectors v_g = g_w - mean(h_w)
    Initialise list θ_list
    for (v_1, v_2) in Combinations(v_g) do
        Add ∠(v_1, v_2) to θ_list
    end
    return θ_list
```

APPENDIX C
NAVIGATION CONDITIONS AND ROUTES

This section elaborates on the design of the conformal and non-conformal symbology, the positioning of the HUD, and on the generation of navigation routes.

A. Conformal symbology

Two conformal navigation conditions were designed based on the works of Narzt et al. [36] and Medenica et al. [34]: one overlaying the road and one above the road, see Figure 13. Although both designs look similar, a small review amongst drivers quickly showed there were substantial differences in opinion regarding the usability of the conditions. All drivers preferred the symbology which was above the road and had similar reasoning as to why. Namely, that projecting symbology in areas regarded as important to drivers i.e., the road, was "*distracting*" or "*annoying*" and felt "*unsafe*" as they felt they had more difficulty seeing what was exactly going on further down the road.

Because of the one-sided criticism on the on-road projections, this design was deemed unfit for experimental use. Therefore, the experiment was conducted using only the conformal symbology above the road, which for the remainder of this section is referred to as the virtual cable.

(a) (b)

Fig. 13: The two conformal symbology designs.

B. Non-conformal symbology

The non-conformal navigation symbology was designed to be simple and easy to read for all types of drivers. Arrow representations of upcoming navigation operations i.e., arrows pointing left, right, or straight, were used, see Figure 14. The symbology was displayed on a HUD; measuring 20 cm high and 25 cm wide; similar to other HUD studies [21, 22, 26]. A review of this system revealed drivers required an indicator as to when they were exactly supposed to turn or go straight. Thus, a distance indicator showing the remaining distance from the upcoming navigation operation was added in white, on the bottom of the HUD.

Fig. 14: Non-conformal symbology: representing a left turn, a right turn, and a straight.

(a) HL condition (b) HH condition (c) VC condition

Fig. 15: The three navigation conditions from participants point of view.

C. Navigation conditions

Three navigation conditions were employed during the experiment, see Figure 15. One using the conformal virtual cable (VC) and two using the non-conformal arrow representations projected on a low positioned HUD (HL) and a high positioned HUD (HH). The high positioned HUD was introduced to overlap the position of the virtual cable in order to exclude possible effects introduced by symbology position. The low HUD was introduced to validate participants use of the high positioned HUD. A high positioned HUD is unconventional and has been shown to be distracting [22]. Therefore, the conventional low HUD position was used to validate whether the unconventional high positioned HUD performed adequately.

The position of the low HUD was based on other HUD studies [21, 22, 26] and was positioned 2.5 m in front of the driver, just above the hood of the vehicle, at a horizontal and vertical angle of 0° and -2.5°, respectively. It was verified that drivers of all heights were able to see the display in full.

The position of the high HUD was set such that it overlapped the virtual cable in the 'perfect' driving situation. No exact overlap was possible because the position of the HUD, relative to the virtual cable, changes depending on the position and orientation of the vehicle since the virtual cable is world-fixed whereas, the HUD is fixed to the vehicle. Therefore, the position of the HUD was based on the assumption that participants would drive centred on the right half of the road (as instructed). Using this position of the vehicle, the high HUD display was configured manually to overlap as much as possible with the position of the virtual cable. This resulted in the following position: 2.5 m in front of the driver, at a horizontal and vertical angle of 3.5° and 20°, respectively.

D. Navigation route

Because repetition of a route may induce some learning effect, four different routes were created: one for each navigation condition and one functioning as a practise route. The routes were designed to last about 6 minutes, containing 26 navigation operations: 12 left turns, 12 right turns and 2 straights. Only two straights were incorporated because navigating straight required almost no action from participants. Reasoning that the differences between the navigation conditions would be less prevalent if many straights would be incorporated only two were added; mainly to interrupt the otherwise monotone left and right turns.

The order of navigation operations was generated by randomly shuffling a list containing 12 left and 12 right turns. Because straights functioned mainly to interrupt the streak of left and right turns, they were inserted in this list afterwards, constrained to be at least 3 operations away from the start, the end, and from each other. The resultant order of navigation operations is shown in Table IV. All participants drove these routes in the following order: practise route, route 1, route 2, and route 3.

TABLE IV: The order of navigation operations per route, each route containing 12 left turns, 12 right turns and 2 straights. Every participant drove these routes in the same order: practise route, route 1, route 2, and route 3.

Index	Practise route	Route 1	Route 2	Route 3
1	Left	Left	Right	Left
2	Left	Left	Left	Left
3	Left	Right	Right	Right
4	Right	Left	Right	Left
5	Left	Left	Left	Left
6	Right	Left	Right	Left
7	Right	Left	Left	Left
8	Right	Left	Left	Right
9	Left	Left	Left	Straight
10	Left	Left	Right	Left
11	Left	Straight	Right	Right
12	Left	Right	Left	Right
13	Straight	Left	Straight	Right
14	Right	Right	Right	Left
15	Right	Right	Left	Left
16	Left	Left	Left	Right
17	Straight	Right	Right	Left
18	Right	Right	Right	Right
19	Right	Right	Straight	Straight
20	Right	Right	Right	Right
21	Left	Straight	Left	Right
22	Left	Right	Left	Left
23	Right	Right	Left	Right
24	Right	Right	Right	Left
25	Left	Left	Left	Right
26	Right	Right	Right	Right

APPENDIX D
SIMULATION TECHNICALITIES

This section will elaborate on simulation environment, the positioning, and detection of visual, and the implementation of the VR glasses. The project is available on this[2] Github repository.

A. Environment

The simulation was build using the Unity Game Engine version 2019.4.3f.1, based on the simulation environment by Bazilinskyy et al. [1], and with the packages listed in Table V. A tool was made such that any navigation route could be driven using this simulation when supplying a navigation route consisting of a list of navigation operations e.g., a list of left turns, right turns and straights, see Appendix C. This navigation route was used to build the environment by positioning and configuring a sequence of intersections dynamically. Each intersection measured 180 by 180 m; an example can be seen in Figure 16. Several different intersections were made to reduce repetitive scenery, using the buildings shown in Figure 18.

Regarding the lighting during the experiment, it was chosen to use a light source shining straight down; with a 90° angle with respect to the ground. This was done to prevent any shadows being cast on parts of the navigation symbology or other important parts of the scene, which may hinder visibility. Furthermore, Unity allows for lights to only be cast on specific objects. This functionality was used to properly light the visual stimuli of the visual search task such that they were equally lit from all sides i.e., no shadow on the lower side of the stimulus due to the sun shining from above.

The lighting rendering mode employed was 'Baked Indirect' which combines real-time direct light-rays and pre-calculated renders for indirect light-rays. This boosts performance compared to doing all lighting calculations in real-time while generating realistic results. The settings used during the experiment are shown in Table V.

TABLE V: Unity packages and lightning settings

Name	Usage / Value
Package	
Town Constructor 3 [3]	Buildings and miscellaneous objects
Pro[4]	Vehicle dynamics and controller
Unlock assets[5]	Vehicle design
VR2Pro-UnityModules[6]	VR glasses
Setting	
Environment resolution	1024
Direct samples	512
Indirect samples	1024
Environment samples	1024
Bounces	4
Lightmap resolution	128
Lightmap Padding	4
Lightmap size	4096

[2]https://github.com/MarcSchotman/mySimulator

(a) Top view of an example intersection

(b) 3D view of an example intersection

Fig. 16: An example of an intersection. A set of these intersections were used to make the route driven by participants.

B. Visual stimuli placement and detection

A total of 75 stimuli were used per navigation route. The stimuli positions were determined using Unity's random number generator and some constraints. The stimuli positions were constrained to the areas depicted in Figure 17, with heights between 0.5 and 2.5 m, and no more than one stimuli per area. Additionally, a minimum of 2 and a maximum of 5 stimuli were presented between each navigation operation e.g., between a left turn and the next right turn. To ensure all participants were shown stimuli at exactly the same positions, the 'seed number' functionality was used. Supplying a seed number to Unity determines the sequence of 'random numbers' generated. Thus, each navigation route was assigned a number (1,2,3,4) which was supplied to Unity's random number generators, resulting in the same 'random' positions of stimuli

[3]https://assetstore.unity.com/packages/3d/environments/urban/town-constructor-3-71070

[4]https://assetstore.unity.com/packages/tools/physics/vehicle-physics-pro-community-edition-153556

[5]https://assetstore.unity.com/packages/3d/vehicles/land/unlock-70s-muscle-car-01-si-104451#content

[6]https://github.com/varjocom/VR2Pro-UnityModules

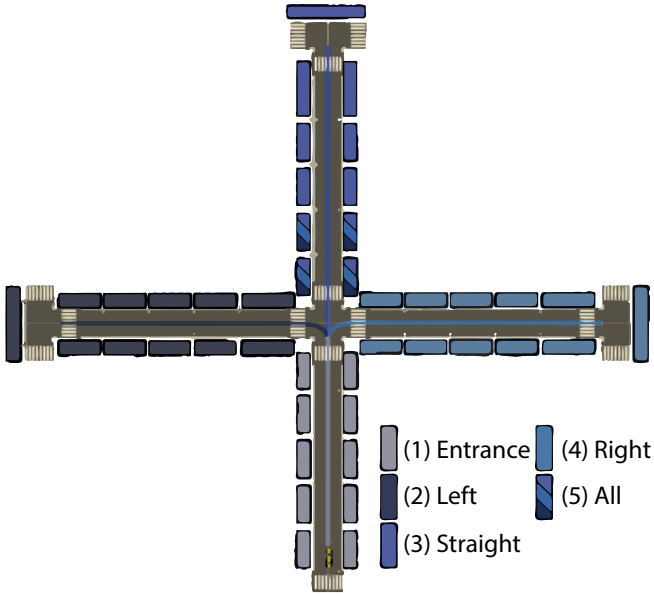

Fig. 17: Spawn locations of visual stimuli for an intersection. Spawn locations were depended on the route, for example, a route going left at the intersection could spawn visual stimuli at the locations corresponding to 1, 2 and 5.

every time a specific navigation route was driven.

To report a detection, participants were required to look at the visual stimulus and press the detection button. After a stimulus was marked as detected it would disappear from the environment functioning as feedback for the participant. Multiple visual stimuli would often be within the field of view of participants, requiring a method for determining which stimulus was being detected. Unity has two functionalities which enabled this differentiation: (1) *ray casting*, using a starting point and direction it returns the first intersection with a simulated object, and (2) *object memory*, allowing individual objects to store data. Using a ray cast with the location of participants and their current gaze direction determined which object was being currently looked at. Additionally, when a visual stimulus was being watched it would log the current timestamp. When participants pressed the detection button the following logic would be set in motion. If a stimulus was being watched at this moment, this stimulus would be marked as detected. Otherwise, loop over all stimuli, selecting the one with the most recent logged timestamp; if this timestamp was less than 0.5 s old then this stimulus was marked as detected. If no stimulus was marked through this process, report a false positive.

C. Varjo implementation and Gaze tracking

The HMD used was developed by Varjo. The implementation in Unity was done using their developed Unity package: VR2Pro-UnityModules[8]. It was accompanied by a multitude of functionalities including data logging, gaze ray casting, and eye-tracking calibration. These functionalities were used without any additions with exception of the data logger, where the vehicle position, vehicle rotation, and object of interest currently being looked at were included. The object of interest being looked at were determined using the ray casting functionality which returns the first simulated object being hit by the current gaze direction.

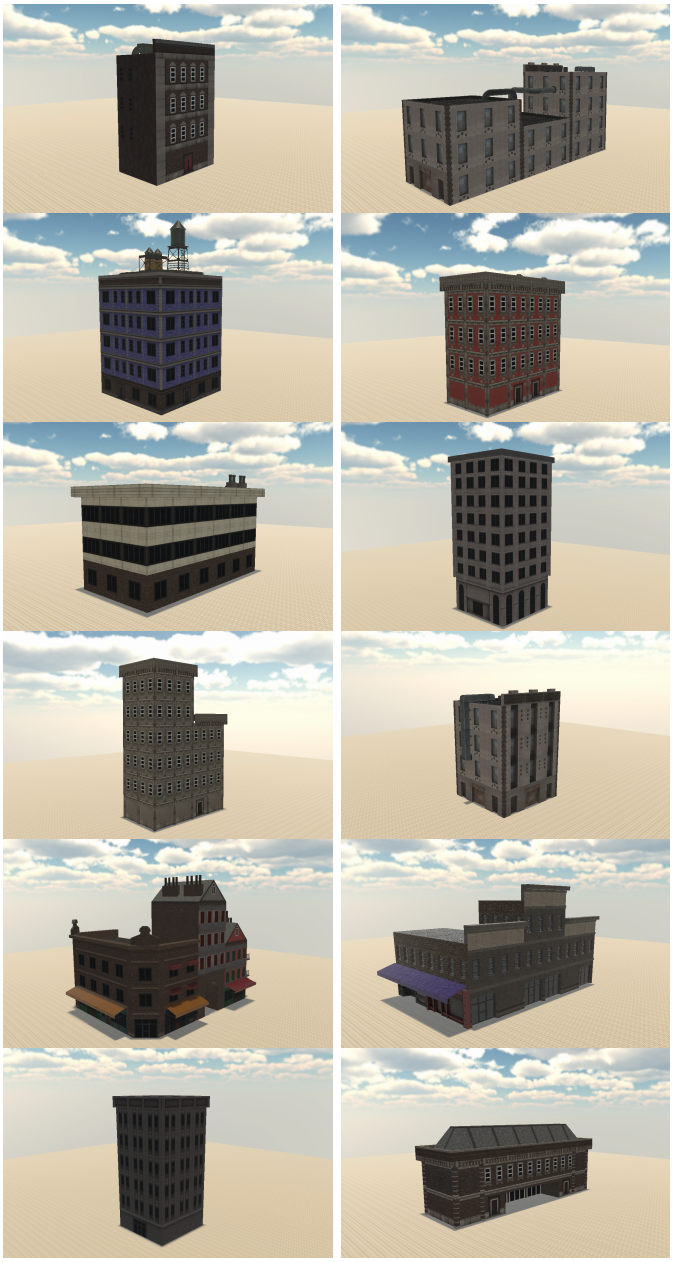

Fig. 18: The houses used to build the different intersections. All buildings can be found in the folder: Assets/_Prefabs/buildings of the unity project of this[7] Github repository.

[8]https://github.com/varjocom/VR2Pro-UnityModules

APPENDIX E
RAW DATA

In this section the raw data of all participants. All figures have the same axis limits for easy comparison between subjects. The first figure contains the horizontal and vertical gaze angles of all fixations across conditions. The second figure shows a histogram of participants' fixations per condition, with the horizontal and vertical gaze angle on the x-axis and the fixation distance on the y-axis with histogram bins of 6° and 10 m for the x- and y-axis, respectively. Calculation of fixation gaze angles and distances can be found in Appendix B. The third figure contains all 9 dependent variables:

(a) The miss rate of stimuli of the secondary visual search task (%)
(b) The reaction time to visual stimuli of the secondary visual search task (s)
(c) The mean saccade length (°)
(d) The mean fixation duration throughout the trial (ms)
(e) The horizontal and vertical spread of fixation (°) i.e., standard deviation of participants' horizontal and vertical fixation gaze angles
(f) The horizontal and vertical gaze speed ($°/s$)
(g) The fixation rate ($\#/s$)
(h) The mean fixation duration on OOI (ms)
(i) The total number of fixations on OOI (#)

A. Participant 1

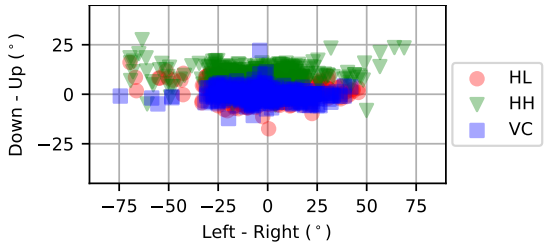

Fig. 19: Fixation angles of participant 1 across conditions.

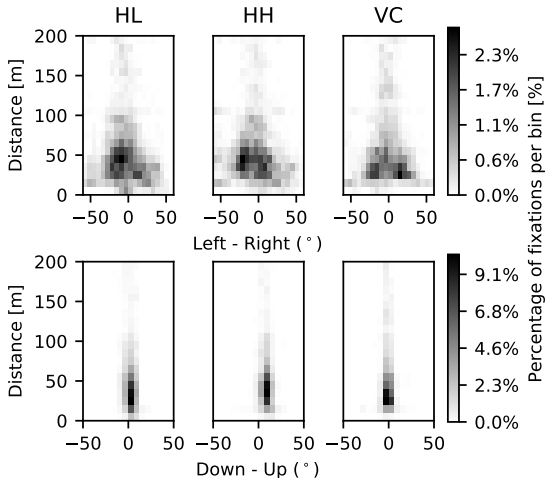

Fig. 20: Histogram of participant 1's fixations across conditions.

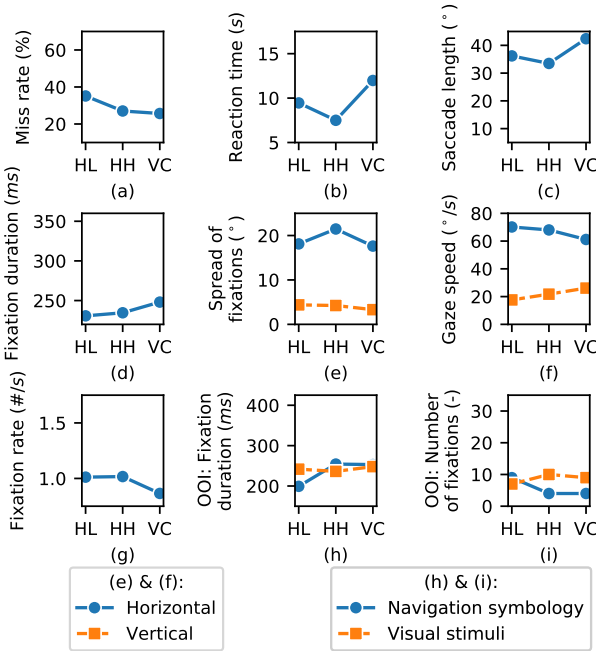

Fig. 21: Dependent variables of participant 1 across conditions.

B. Participant 2

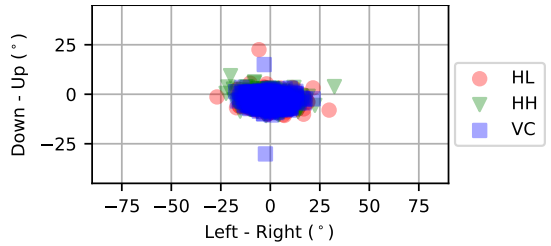

Fig. 22: Fixation angles of participant 2 across conditions.

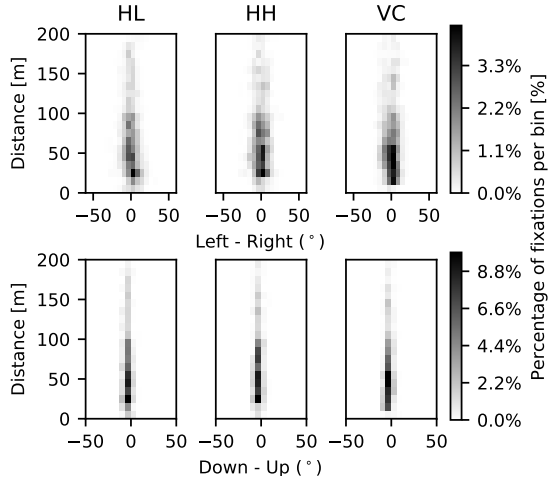

Fig. 23: Histogram of participant 2's fixations across conditions.

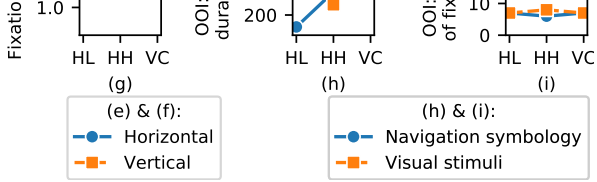

Fig. 24: Dependent variables of participant 2 across conditions.

C. Participant 3

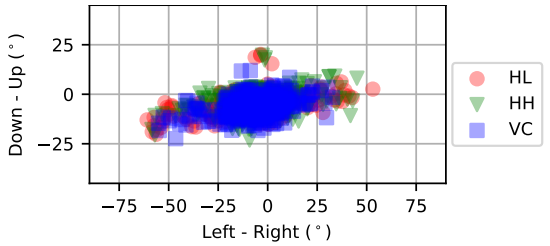

Fig. 25: Fixation angles of participant 3 across conditions.

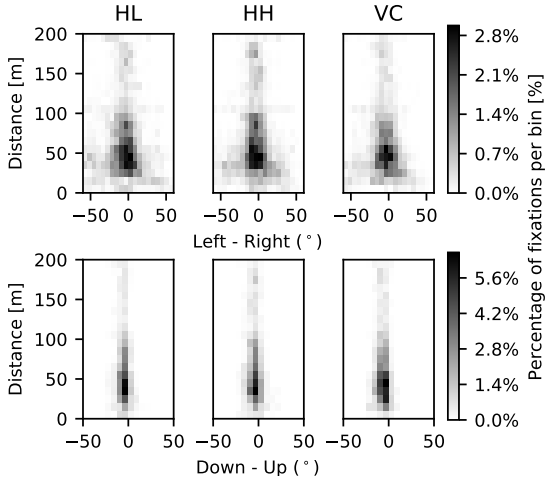

Fig. 26: Histogram of participant 3's fixations across conditions.

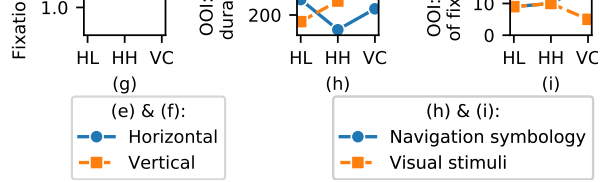

Fig. 27: Dependent variables of participant 3 across conditions.

D. Participant 4

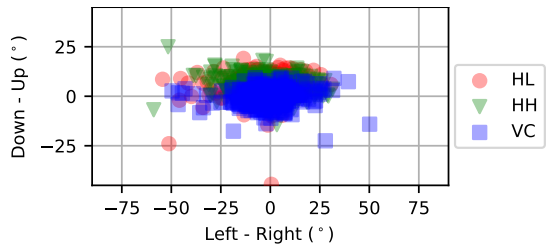

Fig. 28: Fixation angles of participant 4 across conditions.

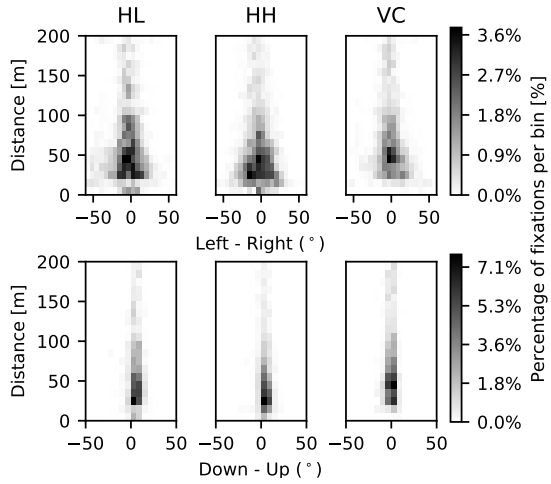

Fig. 29: Histogram of participant 4's fixations across conditions.

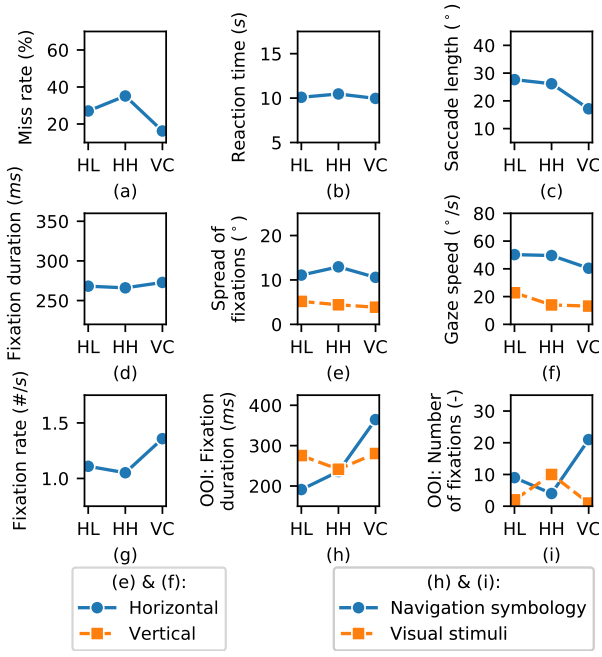

Fig. 30: Dependent variables of participant 4 across conditions.

E. Participant 5

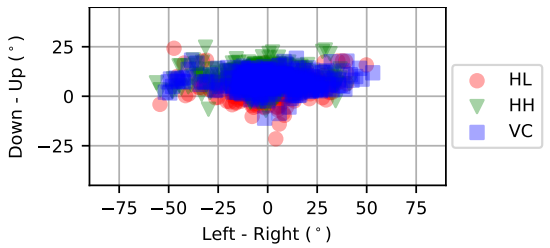

Fig. 31: Fixation angles of participant 5 across conditions.

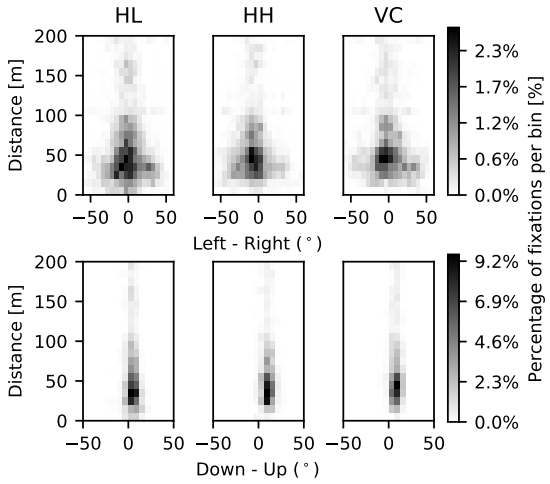

Fig. 32: Histogram of participant 5's fixations across conditions.

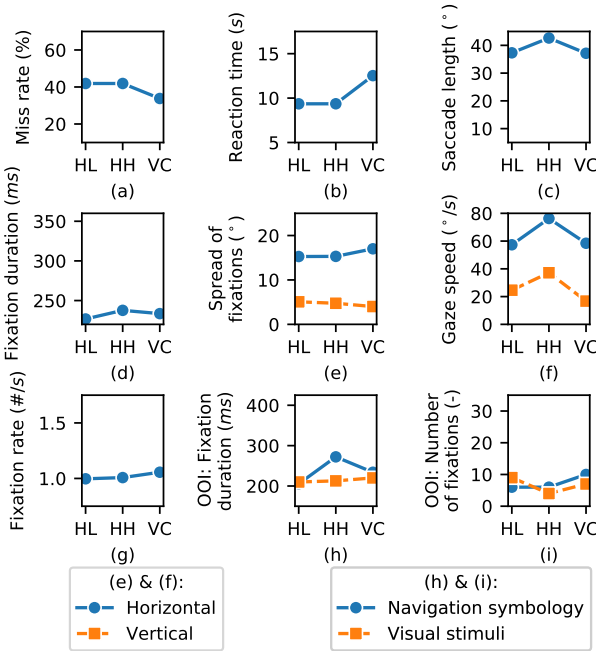

Fig. 33: Dependent variables of participant 5 across conditions.

F. Participant 6

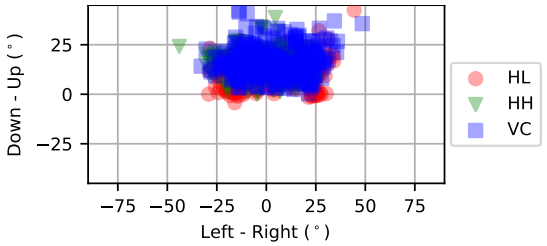

Fig. 34: Fixation angles of participant 6 across conditions.

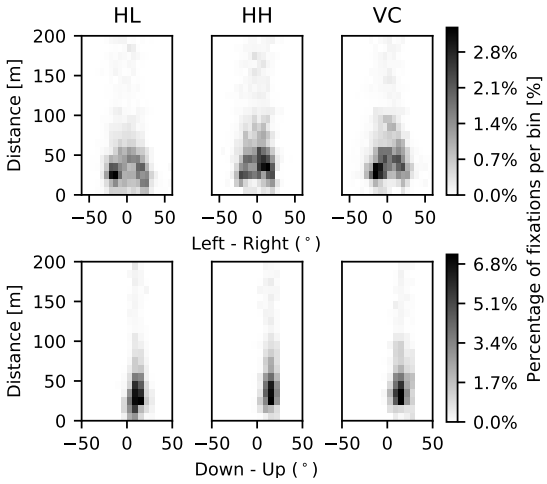

Fig. 35: Histogram of participant 6's fixations across conditions.

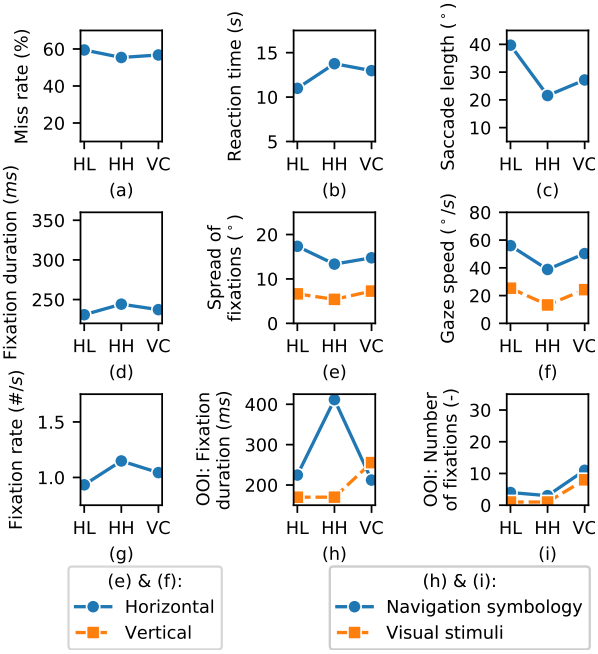

Fig. 36: Dependent variables of participant 6 across conditions.

G. Participant 7

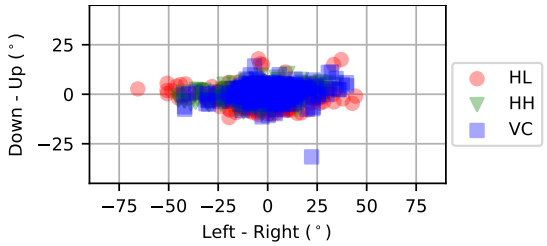

Fig. 37: Fixation angles of participant 7 across conditions.

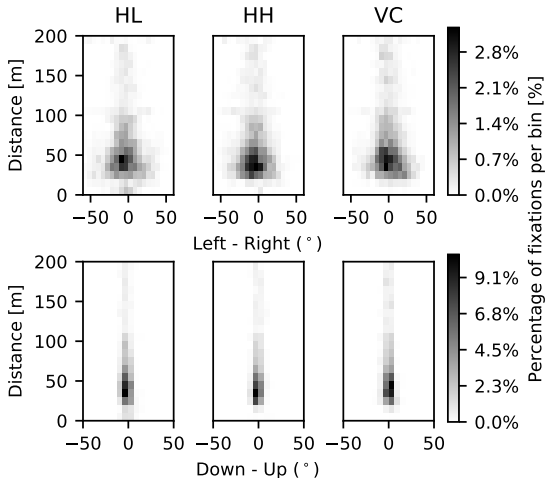

Fig. 38: Histogram of participant 7's fixations across conditions.

Fig. 39: Dependent variables of participant 7 across conditions.

H. Participant 8

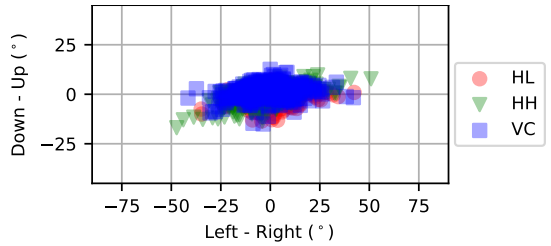

Fig. 40: Fixation angles of participant 8 across conditions.

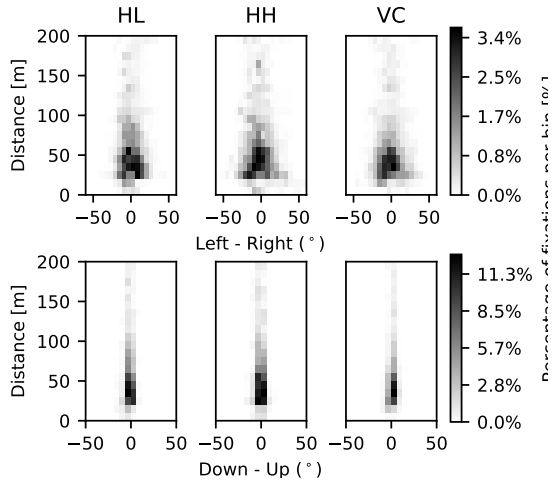

Fig. 41: Histogram of participant 8's fixations across conditions.

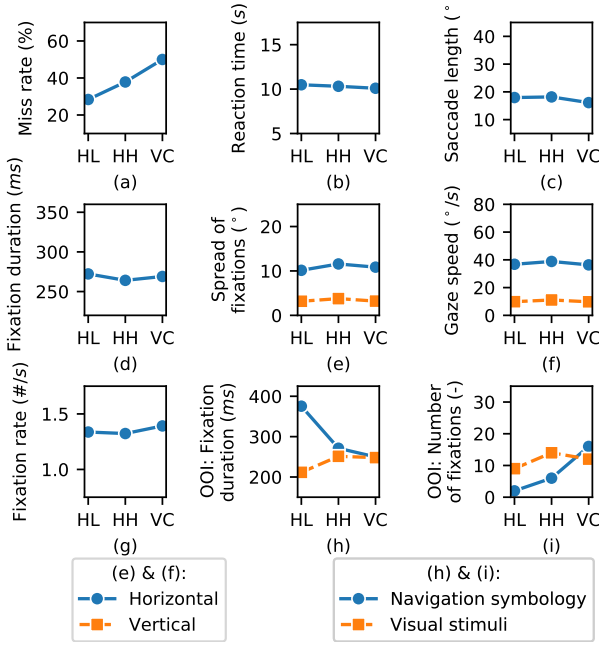

Fig. 42: Dependent variables of participant 8 across conditions.

I. Participant 9

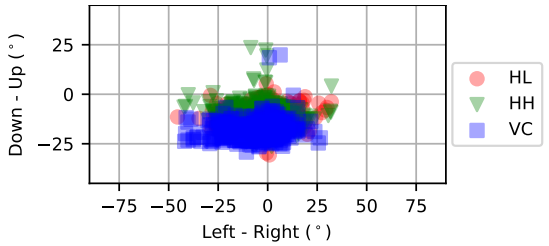

Fig. 43: Fixation angles of participant 9 across conditions.

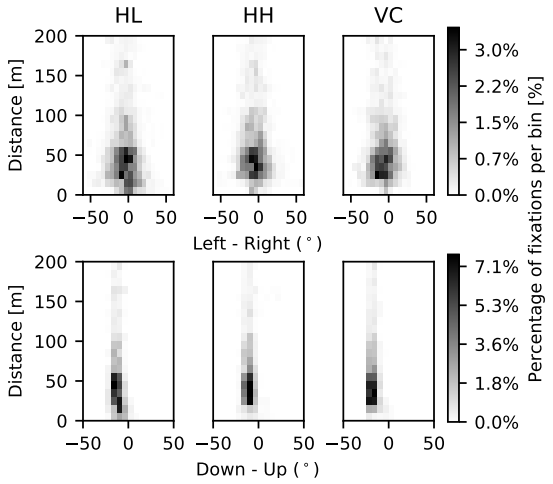

Fig. 44: Histogram of participant 9's fixations across conditions.

Fig. 45: Dependent variables of participant 9 across conditions.

J. Participant 10

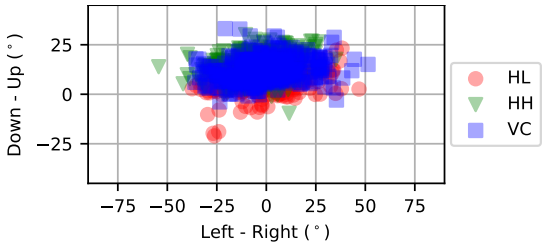

Fig. 46: Fixation angles of participant 10 across conditions.

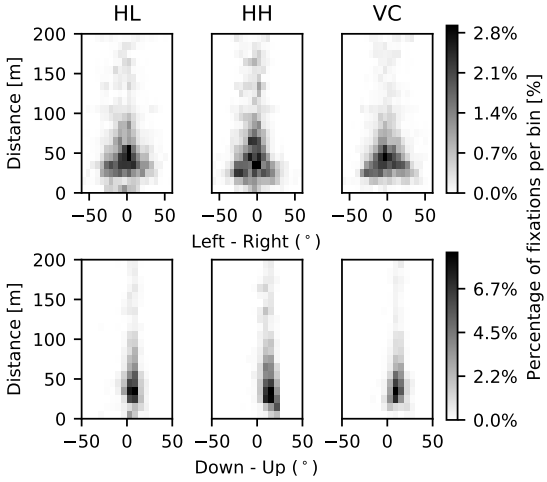

Fig. 47: Histogram of participant 10's fixations across conditions.

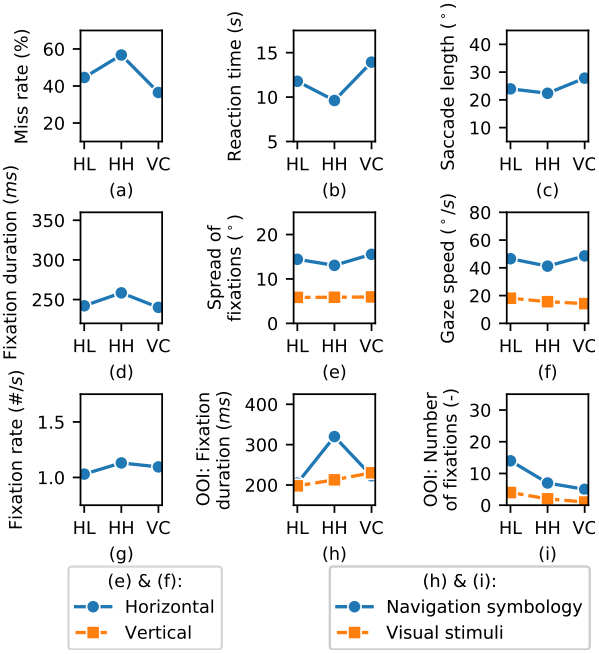

Fig. 48: Dependent variables of participant 10 across conditions.

K. Participant 11

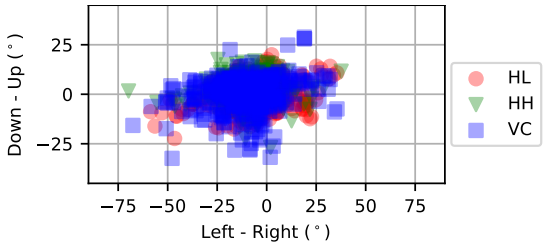

Fig. 49: Fixation angles of participant 11 across conditions.

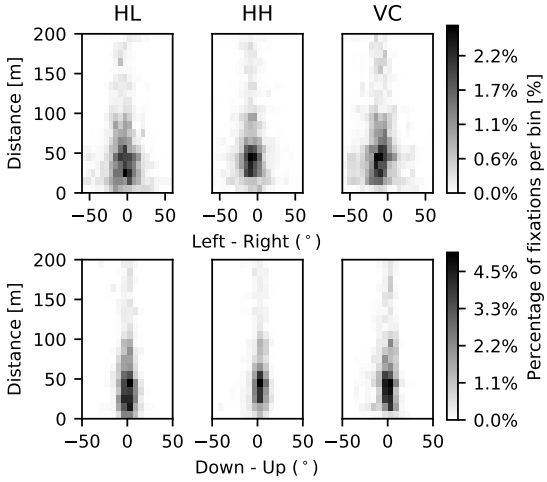

Fig. 50: Histogram of participant 11's fixations across conditions.

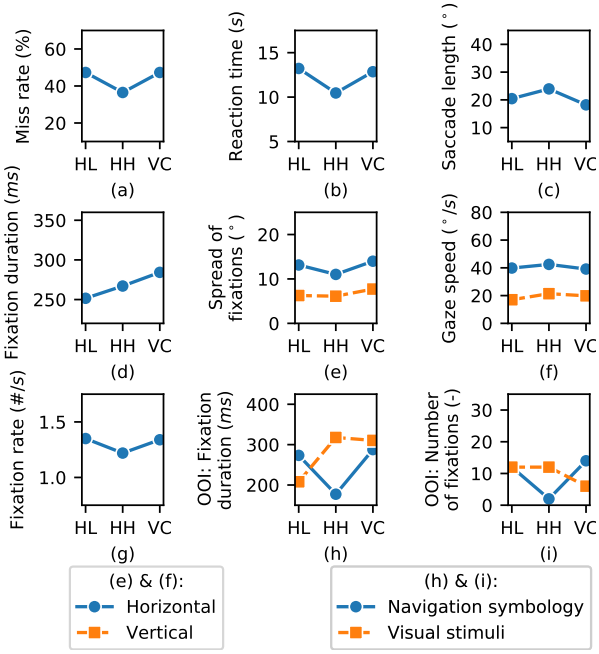

Fig. 51: Dependent variables of participant 11 across conditions.

L. Participant 12

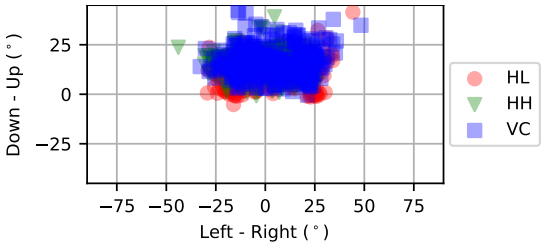

Fig. 52: Fixation angles of participant 12 across conditions.

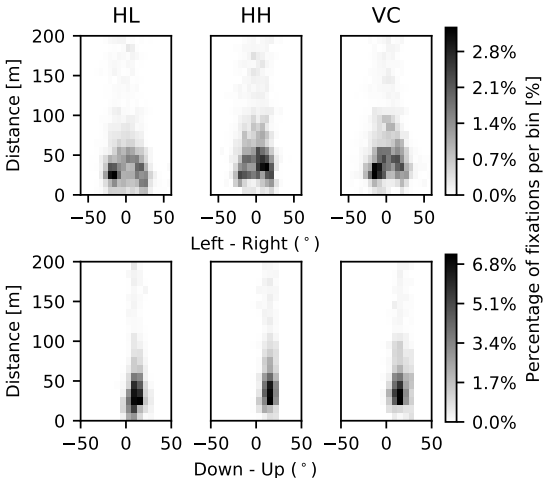

Fig. 53: Histogram of participant 12's fixations across conditions.

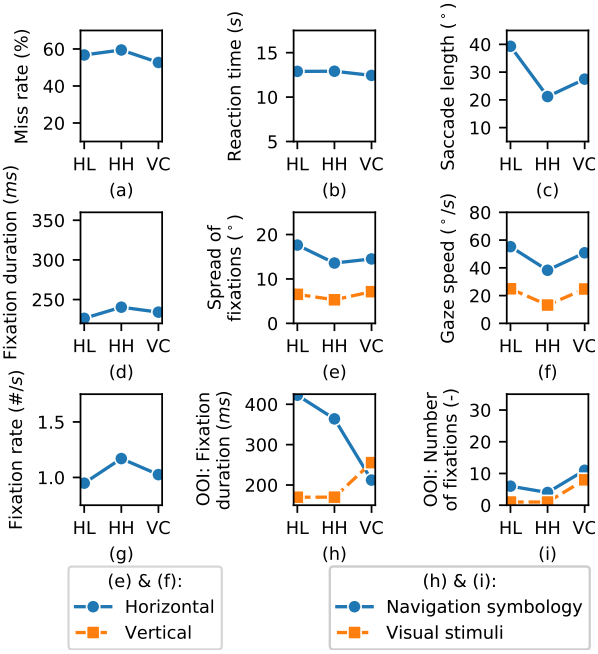

Fig. 54: Dependent variables of participant 12 across conditions.

M. Participant 13

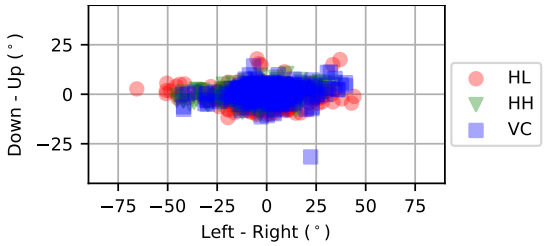

Fig. 55: Fixation angles of participant 13 across conditions.

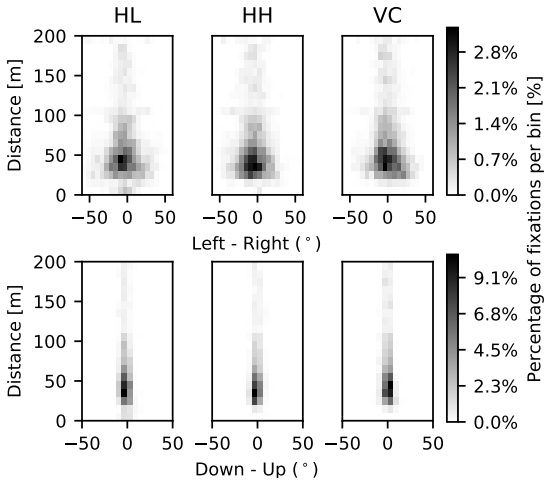

Fig. 56: Histogram of participant 13's fixations across conditions.

Fig. 57: Dependent variables of participant 13 across conditions.

N. Participant 14

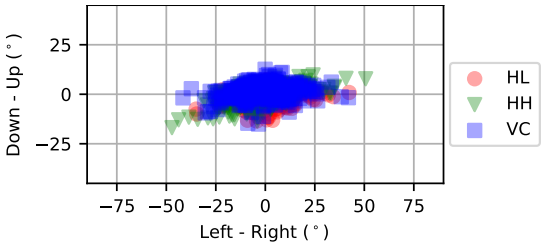

Fig. 58: Fixation angles of participant 14 across conditions.

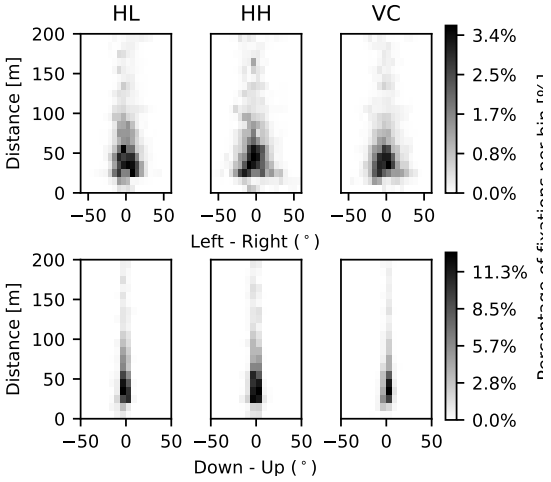

Fig. 59: Histogram of participant 14's fixations across conditions.

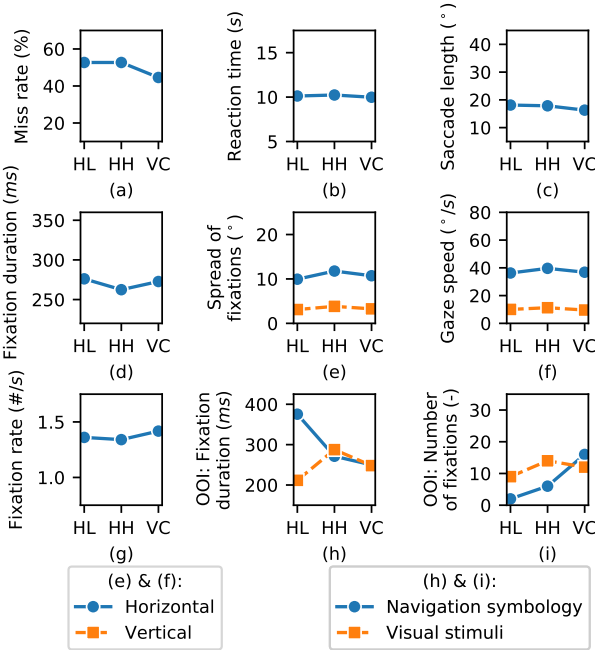

Fig. 60: Dependent variables of participant 14 across conditions.

O. Participant 15

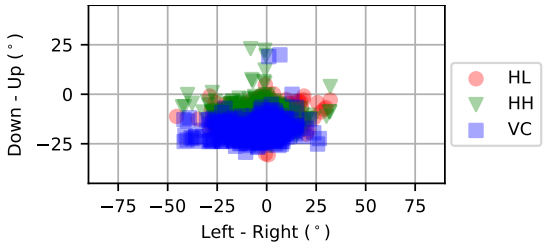

Fig. 61: Fixation angles of participant 15 across conditions.

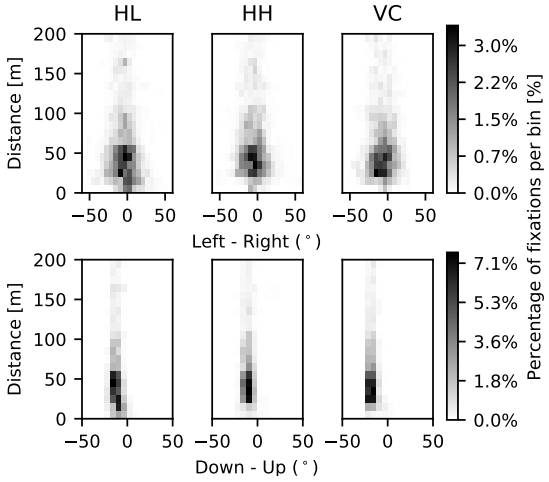

Fig. 62: Histogram of participant 15's fixations across conditions.

Fig. 63: Dependent variables of participant 15 across conditions.

P. Participant 16

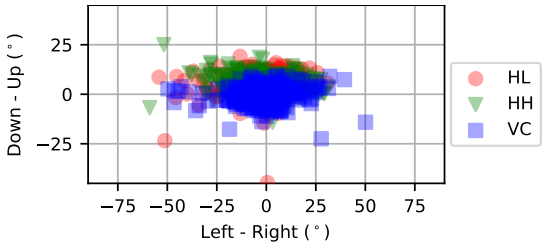

Fig. 64: Fixation angles of participant 16 across conditions.

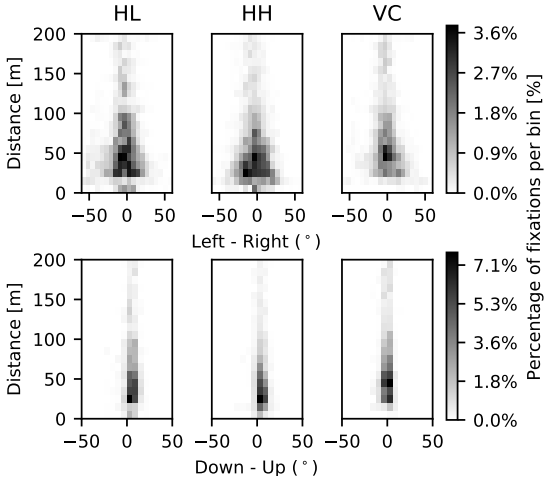

Fig. 65: Histogram of participant 16's fixations across conditions.

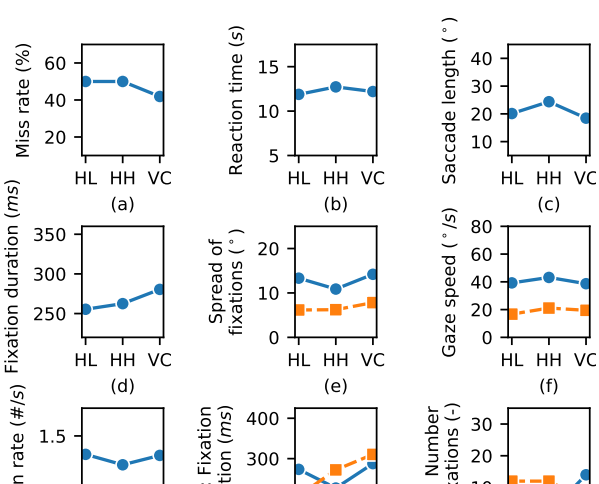

Fig. 66: Dependent variables of participant 16 across conditions.

Q. Participant 17

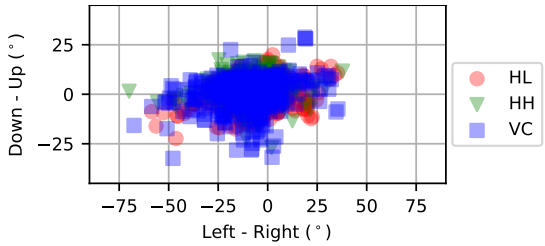

Fig. 67: Fixation angles of participant 17 across conditions.

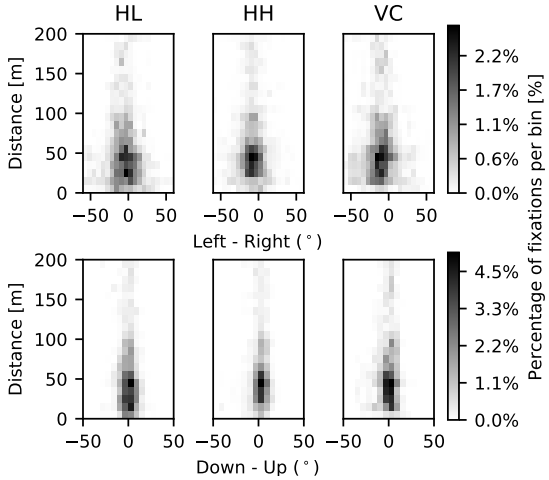

Fig. 68: Histogram of participant 17's fixations across conditions.

Fig. 69: Dependent variables of participant 17 across conditions.

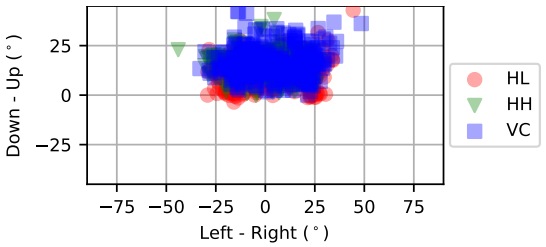

Fig. 70: Fixation angles of participant 18 across conditions.

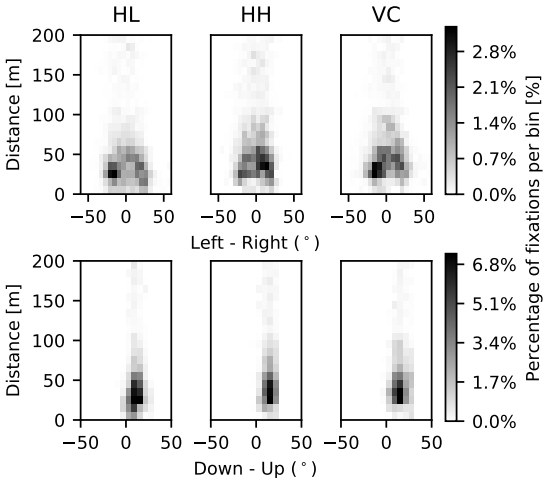

Fig. 71: Histogram of participant 18's fixations across conditions.

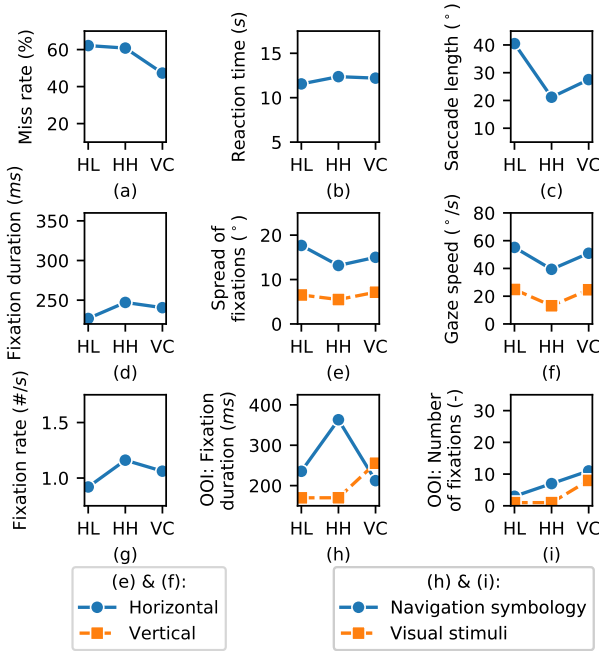

Fig. 72: Dependent variables of participant 18 across conditions.

APPENDIX F
FORMS

This appendix contains all used forms through-out the experiment. Before the start of the experiment participants read and signed the informed consent form, shown in section A. Then, they filled in a brief questionnaire containing demographic and driving related questions, shown in section B. Thereafter, they were asked to read the experimental instructions, shown in section C. These instructions were also communicated verbally. Finally, after each experimental trial they filled in the MISC and van der Laan questions shown in section D.

Researchers:

MSc Student: M.A. Schotman
E-mail: M.A.Schotman@student.tudelft.nl
Tel: +31 (0)6 535 022 98

Supervisor: Dr.ir. J.C.F. de Winter
E-mail: j.c.f.dewinter@tudelft.nl

Supervisor: Ir. Y.B. Eisma
E-mail: Y.B.Eisma@tudelft.nl

This document describes the location, purpose of the research, preventative measures related to COVID-19, procedures of the experiment, risks of participating, the right to withdraw, and data anonymity. Please read all sections carefully and answer the questions on page 2.

Location of the experiment

TU Delft, Faculty of Mechanical, Maritime and Material Engineering.
Department of Cognitive Robotics
Mekelweg 2, 2628 CD, Delft
Room F-0-220 CoR Lab

Purpose of the research

The purpose of this research is to investigate the effect of navigation symbols on your gazing behavior and visual search performance. The results of the study may be useful for designing future augmented reality navigation systems and may provide insight into the effects that current navigation systems have on drivers. Both subjective and objective measure will be gathered, analyzed, and published in a MSc thesis and derivative works.

Prevention of the spread of COVID-19

To minimize the risk of COVID-19, you may not participate if you:

- Show symptoms indicative of COVID-19
- Have been in contact with COVID-19 patients within the last 14 days
- Are over the age of 65

The following preventative measures will be required for you to participate:

- Wash your hands thoroughly before entering the lab
- Keep at least 1.5 meters from the researcher and other people inside the lab.
- Wear a face mask when in the lab (provided by us if needed).

Procedure

During the experiment, you will wear a head-mounted virtual reality glass and use a steering wheel to control the simulated vehicle (the speed of the vehicle will be controlled automatically). Before the experiment starts, you will drive a test round to assess your risk of simulation sickness and to get familiarized with the experimental equipment, driving controls, visual search task, and the navigation symbols. After the test drive is successfully completed, the experiment will start. The experiment will consist of several trials, each with different navigation symbols conditions and a secondary visual search task.

Risk of participating

Virtual environments and the use of virtual reality glasses can cause motion sickness which can manifest itself in different ways: visuomotor dysfunctions (eyestrain, blurred vision, difficulty focusing), nausea, drowsiness, fatigue, or headaches. If you experience any discomfort, please inform the experimenter so the simulation can be stopped. You may take off the headset any time if you feel unwell.

Procedure for withdrawal from study

Your participation is completely voluntary, and you may stop at any time during the experiment. Either ask the experimenter to stop the simulation and help you take off the headset or take off the headset yourself. There will be no negative consequences for withdrawing from the experiment.

Data confidentiality

All data collected during the experiment will be stored anonymously and used for the purpose of academic research only. When used in publications, all gathered data will be anonymous.

Please answer the following questions:	**Yes**	**No**
I consent to voluntarily participate in this study	○	○
I have read and understood the information provided in this document.	○	○
I adhere to the preventative measures with regards to COVID-19 as explained on page 1.	○	○
I understand that participation in this study is at my own risk and may cause nausea, drowsiness, fatigue, or headaches.	○	○
I understand that I can withdraw from the study at any time without any negative consequences.	○	○
I consent that all data gathered during the experiment may be used for a Master thesis and possible future academic research.	○	○

Name:

Date:

Signature: _____

1. Age

_____

2. Sex

Mark only one oval.

- ◯ Male
- ◯ Female

3. How many years do you have your drivers licence

Mark only one oval.

- ◯ 0 - 5
- ◯ 5 - 10
- ◯ 10+

4. How often do you drive?

Mark only one oval.

- ◯ Never
- ◯ Rarely - a few times a year
- ◯ Regularly - 1 or 2 times a week
- ◯ Often - more than twice a week

5. How experienced are you with using head-up displays in the car?

Mark only one oval.

- ◯ Never used a HUD
- ◯ Have used it a couple of times
- ◯ Have used it regularly in the past
- ◯ Using it regularly at this moment

This experiment investigates the influence of navigation type and position on drivers' visual search capacity and gazing patterns. You will drive several blocks with different navigation types and perform a visual search task with the VR headset. Your eyes will be tracked by the VR headset.

Your tasks during experiment

1. **Press one of the steering wheel buttons when you see a target (yellow transparent sphere)**
2. **Follow the navigation**

Note: Only press once when you see a target.
Note: Look directly at the target before you press the steering wheel button
Note: Throttle is automated, you only have to steer.
Note: When you make an incorrect turn or drive onto the sidewalk the experiment will reset you position and continue automatically.

Experiment schedule

The experiment will go as follows:

1. **Calibration:** We will start by calibrating your head position with respect to the steering wheel and setting up the eye-tracker. You will be able to try out the steering wheel buttons and your eye-tracking will be visualized.
2. **Practice drive:** You will drive a practice round, try to detect the targets alongside the road and follow the navigation. The goal here is to familiarize you with:
   - The steering mechanics
   - The target detection buttons
   - The different navigation symbology's
3. **A** (optional) **brake**
4. **The experiment:** 6 rounds of about 3 to 4 minutes.
   - Each round will be driven with *a single navigation symbology*
   - Each round will have *a single target difficulty* (easy/hard)
   - After every round you will take off the headset to have a small brake fill in a questionnaire
   - At the beginning of the next round we recalibrate the eye tracking and start again.

1. Please indicate your MISC score

Alert the experiment supervisor when your score is 4 or higher

Mark only one oval.

- ◯ 0 - No problems
- ◯ 1 - Uneasiness (no typical symptoms)
- ◯ 2 - Vague dizziness, warmth, headache, stomach awareness, sweating..
- ◯ 3 - Slight dizziness, warmth, headache, stomach awareness, sweating..
- ◯ 4 - Fairly dizziness, warmth, headache, stomach awareness, sweating..
- ◯ 5 - Severe dizziness, warmth, headache, stomach awareness, sweating..
- ◯ 6 - Slight naussea
- ◯ 7 - Fairly naussea
- ◯ 8 - Severe naussea
- ◯ 9 - (near) retching naussea
- ◯ 10 - Vomiting

2. I find this navigation condition to be

Mark only one oval.

	1	2	3	4	5	
Usefull	◯	◯	◯	◯	◯	Useless

3. I find this navigation condition to be

Mark only one oval.

	1	2	3	4	5	
Pleasant	◯	◯	◯	◯	◯	Unpleasant

4. I find this navigation condition to be

Mark only one oval.

	1	2	3	4	5	
Bad	◯	◯	◯	◯	◯	Good

5. I find this navigation condition to be

Mark only one oval.

	1	2	3	4	5	
Nice	◯	◯	◯	◯	◯	Annoying

6. I find this navigation condition to be

Mark only one oval.

	1	2	3	4	5	
Effective	◯	◯	◯	◯	◯	Superfluous

7. I find this control condition to be

Mark only one oval.

	1	2	3	4	5	
Irritating	◯	◯	◯	◯	◯	Likable

8. I find this navigation condition to be

Mark only one oval.

	1	2	3	4	5	
Assisting	◯	◯	◯	◯	◯	Worthless

9. I find this navigation condition to be

Mark only one oval.

	1	2	3	4	5	
Undesirable	◯	◯	◯	◯	◯	Desirable

10. I find this navigation condition to be

Mark only one oval.

	1	2	3	4	5	
Raising alertness	◯	◯	◯	◯	◯	Sleep-inducing

11. Please, feel free to share any thoughts regarding this condition